Measurement of Snowfall by Optical Attenuation

by

C. Warner

M.Sc. Thesis. Department of Meteorology, McGill University

ABSTRACT

A transmissometer has been used to provide a continuous record with good time resolution of falling snow. The pulsed light, of wavelength 0.45 μ traversed a path 71 m long about 20 m above ground level. A total snow amount of 160 millimeters of water was recorded from 18 storms through the 1966-67 winter season. Attenuation by snow was found to be proportional to rate of snowfall, with the constant of proportionality 11 (db km^{-1})/(mmw hr^{-1}). A previous experiment by Lillesaeter yielded 18 for this constant. His higher value is probably due in large part to the effect of thermal fluctuations on his narrower transmitted beam.

Snow amounts per storm deduced from attenuation records agreed with amounts measured by standard instruments to within a factor 2. When depths on the ground were compared, agreement was within a factor 1.5.

Observations on the variation of "clear air" attenuation with humidity are included in an appendix.

MEASUREMENT OF SNOWFALL BY OPTICAL ATTENUATION

by

C. Warner

A thesis submitted to the Faculty of Graduate Studies and Research in partial fulfilment of the requirements for the degree of Master of Science

Department of Meteorology
McGill University
Montreal

June 1967

TABLE OF CONTENTS

ABSTRACT

A transmissometer has been used to provide a continuous record with good time resolution of falling snow. The pulsed light, of wavelength 0.45 μ traversed a path 71 m long about 20 m above ground level. A total snow amount of 160 millimeters of water was recorded from 18 storms through the 1966-67 winter season. Attenuation by snow was found to be proportional to rate of snowfall, with the constant of proportionality 11 (db km^{-1})/(mmw hr^{-1}). A previous experiment by Lillesaeter yielded 18 for this constant. His higher value is probably due in large part to the effect of thermal fluctuations on his narrower transmitted beam.

Snow amounts per storm deduced from attenuation records agreed with amounts measured by standard instruments to within a factor 2. When depths on the ground were compared, agreement was within a factor 1.5.

Observations on the variation of "clear air" attenuation with humidity are included in an appendix.

ACKNOWLEDGEMENTS

I am happy to acknowledge the cheerful assistance of almost every member of the Stormy Weather Group during the course of this work. I am grateful to my supervisor, Professor K.L.S. Gunn, and to Professor J.S. Marshall for their guidance and very substantial help. The electronic circuitry was developed by Doctor Marceli Wein and Professor Gunn, and updated by Mr. Ernest Ballantyne. Mr. Isztar Zawadski made many valuable suggestions. Mr. Zygmunt Golstajn did routine maintenance and clerical work throughout the whole period of operation of the transmissometer, and his skill with hardware also was of the greatest value. Mrs. Evelyn Pearl assisted with analyses and Miss Ursula Seidenfuss and Mr. Steven Lapczak prepared diagrams for the thesis. Finally I would like to thank Miss Arlene and Miss Suzette Milburn for their patience and skill in typing the manuscript.

LIST OF FIGURES

1. Introduction

Current standard methods of measuring snowfall quantities leave something to be desired. McGill Observatory is equipped with standard instrumentation for measuring snowfall (Fig. 1), which has been modified in recent years. The Nipher gauge is a simple cylindrical can of 4 inches diameter mounted 6 feet above the ground surface, protected by a surrounding Nipher wind screen. There are two Department of Transport tipping bucket rain gauges, also mounted at a height of 6 feet. Insulation and thermostat-controlled heaters have been added to both of these gauges to maintain the receiving funnel surfaces a few degrees above zero Centigrade so as to render them capable of measuring snowfall rates. Around each has been fitted an Alter wind shield. From April 1966 a precipitation sensor also has been in use at the Observatory, designed to register the beginnings and endings of periods of precipitation.

Even with this relatively sophisticated equipment there has remained doubt after the passage of a snowstorm as to both the total water equivalent of the snow that has fallen (expressed in millimetres of melted water, mmw, or hundredths of an inch), and also the distribution over the time period of the storm of the rate of accumulation. The doubt is due chiefly to the unknown effect of wind flow around the instruments even with the shielding, and to the occurrence of evaporation from the warm receiving surface of the tipping bucket gauges.

In the process of evolving improved methods for measuring snowfall, experiments to detect both the scattering and the attenuation of light due to snowfall have been performed on the McGill campus.

Significant progress was made in a study of attenuation of light in a nearly parallel beam two winters ago (Lillesaeter 1965). However, the equipment came into operation only towards the end of the snow season, and a total of only 49 mmw was recorded. The work described here has been an amplification and extension of that of Lillesaeter. The whole winter snowfall of 1966-67 was recorded, amounting to about 180 mmw, of which about 160 mmw was used for analysis.

In Lillesaeter's experiment the light beam was kept sufficiently narrow that the receiver intercepted nearly all the light transmitted over the 123 m path. This required great stability in the mounting of the equipment. The light beam was transmitted from a heated room into the cold winter air; the turbulence at the boundary led to fluctuations in the position of the beam and so in the recorded signal.

The principal differences between Lillesaeter's equipment and that used in 1966-67 were the mounting of the transmitter outdoors, and the use of a light beam that was considerably broader at the receiver so that slight disturbances to alignment would not affect the recorded signal.

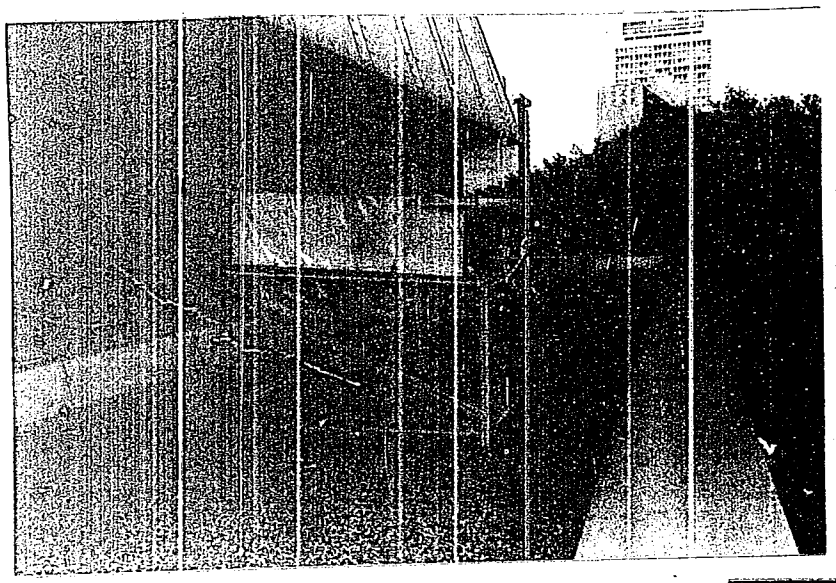

TRANSMITTER

RECEIVER

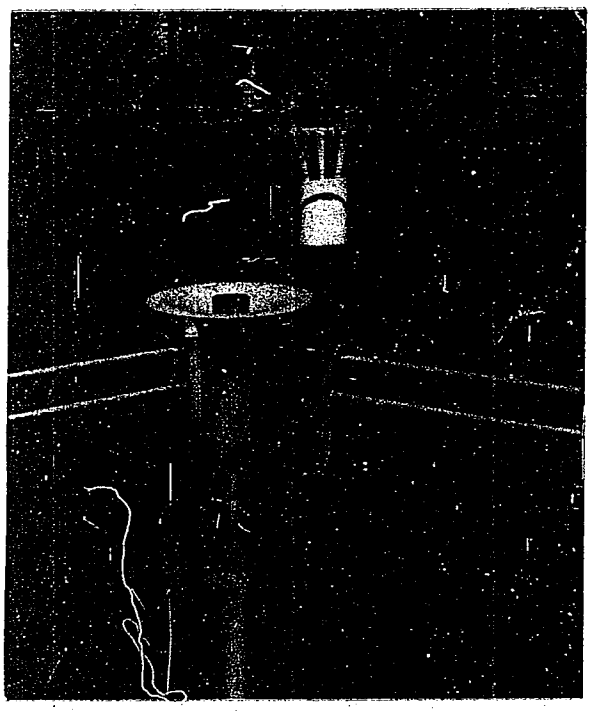

TIPPING BUCKET GAUGE

NIPHER GAUGE

Fig. 1

RECEIVER

TIPPING BUCKET GAUGE

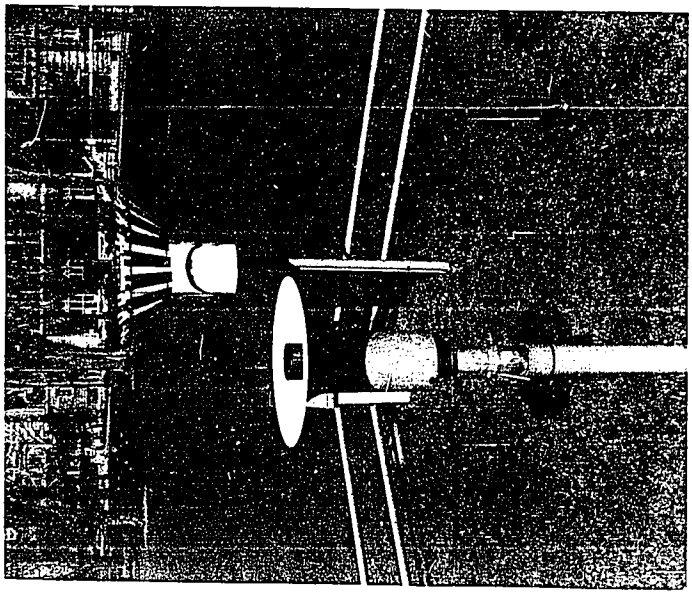

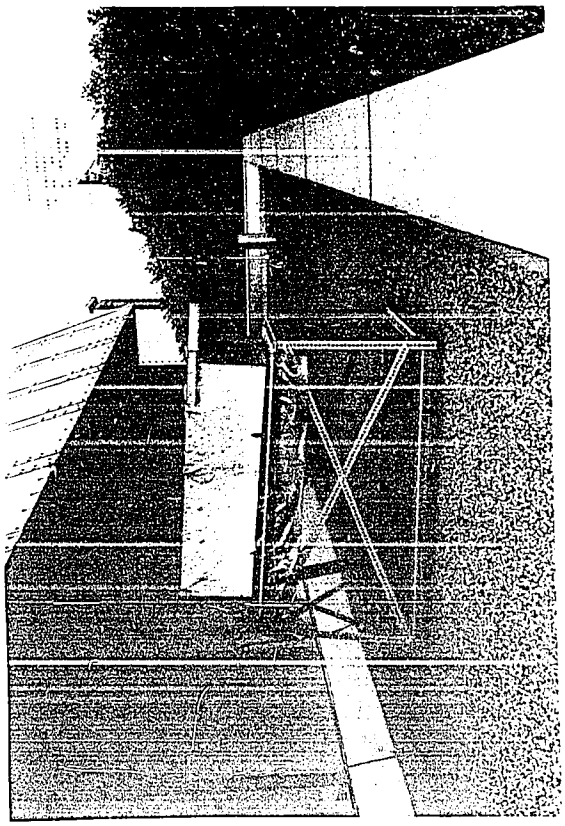

TRANSMITTER

NIPHER GAUGE

Fig. 1

2. Theory of Attenuation of Light

General atmospheric conditions

A flux per unit cross section F of light energy travelling along a path a short distance dx will be diminished or attenuated by an amount given by

$$dF = -F\sigma\, dx \qquad (1)$$

Here σ is the attenuation coefficient, or extinction coefficient, appropriate to the medium through which the light passes. It may be divided into scattering and absorption components, arithmetically summed, due to various types of particles. Integration of equation (1) gives

$$F = F_o \exp(-\sigma x) \qquad (2)$$

The signal level in decibels at any distance relative to the signal level at zero distance is given by

$$10 \log_{10}(F/F_o) = -4.34\sigma x \qquad (3)$$

If attenuation is reckoned from zero at distance zero upwards towards a positive value at the receiver of a transmissometer, the sign may be changed, and for the total effect the following relation may be written:-

$$k = 4.34\,\sigma \qquad (4)$$

where k is the attenuation per unit path length. It is seen that for a fixed path length k depends only upon the attenuation coefficient for the medium.

Atmospheric attenuators of visible light are air molecules, gaseous and particulate pollutants, haze and fog droplets, rain and snow, with total attenuation coefficient components of relative importance given inversely by the stated order, except that a rain shower generally will produce a smaller attenuation than a heavy haze or a fog.

For scattering of light of wavelength (λ) by small particles of diameter (D), three regimes may be distinguished. Where D is less than λ, Rayleigh scattering occurs. This applies to haze in the atmosphere. As D becomes equal to λ the amount of light scattered per particle increases markedly. This is described by the Mie theory of scattering. Where D is greater than λ the field of geometrical shadowing has been reached.

The light source used had its peak intensity near 0.45 μ. Stewart and Hopfield (1965), quoting Deirmendjian (1962), give theoretical values of the attenuation coefficient for light of wavelength 0.45 μ, traversing two types of ordinary light haze, as follows:-

Continental haze (2300 particles cm^{-3}) $\sigma = 0.12\ km^{-1}$; $k = 0.52\ db\ km^{-1}$

Maritime haze (100 particles cm^{-3}) $\sigma = 0.11\ km^{-1}$; $k = 0.48\ db\ km^{-1}$

Values of k have been added, using equation (4). Attenuations commonly measured with snow falling over the 71-m path have been of the order of 10 db km^{-1}. Thus in the observation of variations in time of attenuation by snowfall, the effects of changes of air density and light haze safely may be neglected.

It remains to examine the effects of heavier urban haze and fog. For liquid droplets and dilute solution droplets involving

hygroscopic materials of the urban atmosphere it is satisfactory to assume that scattering is of much greater importance for attenuation of light than is absorption (see, for example, Fig. 14 of the article of Stewart and Hopfield, 1965).

For light of wavelength 0.45 μ, a small haze droplet shows a marked increase of scattering cross section as its size is increased through approximately 0.3 μ. Stewart and Hopfield (1965), who quote from Van de Hulst (1957), and Middleton (1952) discuss this effect of Mie scattering. General treatment of "clear air" attenuation appears in Appendix 1. The important conclusion emerges that as the relative humidity of the atmosphere increases, the transmission in an urban atmosphere of light of wavelength 0.45 μ will decrease, and a marked change is to be expected as the humidity passes the 80% level, owing to the involvement of suddenly increased numbers of hygroscopic nuclei. (The simplifying assumption is made in this treatment that particulates and inhomogeneities in droplets may be ignored.) The possibility of using light of higher wavelength is considered in chapter 5.

The atmospheric effect described constituted the source of greatest uncertainty in interpretation of the experimental results with snowfall, and probably is an inherent limitation in the measurement of snowfall by a transmissometer.

In fog, typical drop-size spectra overlap the size range of the transitional Mie scattering regime for visible light. Furthermore, fogs exhibit processes of evolution. Authoritative treatments of the resulting complexities of attenuation of light in fog are given by Arnulf et al (1957) and by Eldridge (1966). Since in general fog and snow do not occur simultaneously, no further discussion is attempted here.

Attenuation by falling snow

Snow particles have dimensions generally measurable in millimetres; they are large compared with a wavelength = 0.45 μ. For such particles, if effects of diffraction are ignored, the ratio of the area of the wavefront acted upon by the particle to the area of the particle itself - the particle scattering area ratio - approximates to a value constant at 2 (see Middleton, 1952). Thus for snow particles of cross section (a) measured normal to the flux of light, at number density (N), the attenuation coefficient for snow may be expressed approximately as $\sigma_s = (2aN)$. For the attenuation per unit path length due to falling snow we obtain from equation (4) the relation

$$k_s = 4.34\ (2aN)$$

The attenuation due to snowfall depends only on the product (aN). [With a number (q) of different types of snow crystals this product is rewritten in the form $\sum_{i=1}^{\infty} a_i N_i$]

The nature of the relationship between the attenuation per unit path length (k) and the rate (R) of accumulation of melted water due to falling snow is examined in the following paragraphs, using these notations:-

Average particle projected cross-section . . . . . a

Particle mass. . . . . m

Droplet diameter to which particle will melt . . . . . D

Particle fall velocity V

Particle number density in the size range (a) to (a+da). . . N_a

Using the double hyphen to indicate a proportionality rela-

tionship, then with α and β as unknown indices, assumptions as follows may be made:

$$k \text{ ——— } \int_o^\infty a\, N_a\, da$$

$$R \text{ ——— } \int_o^\infty m\, V\, N_a\, da$$

$$m \text{ ——— } a^\alpha$$

$$V \text{ ——— } m^\beta;$$

also $$m \text{ ——— } D^3$$

These may be reduced to give:-

$$k \text{ ——— } \int_o^\infty a\, N_a\, da$$

and $$R \text{ ——— } \int_o^\infty a^{\alpha(\beta+1)} N_a\, da$$

It is seen that if there is an independent relationship between k and R separately, then this will be linear; necessary for this is that

$$\alpha\ (\beta + 1) = 1$$

This condition is satisfied if $\alpha = 1$ and $\beta = 0$; that is if the particle mass is proportional to the projected cross section, and if the fall velocity is constant.

Langleben (1954) found that for aggregate flakes

$$V \text{ ——— } D^{0.31}.$$

From above,

$$V \text{ ——— } D^{3\beta}.$$

Thus for aggregate flakes $\beta \sim 0.1$, and $(\beta + 1) \sim 1$. For perfectly spherical particles $\alpha = 3/2$; for irregularly shaped crystals falling with their largest dimensions on the average lying more nearly in a

horizontal than in a vertical plane, it may be expected that $\alpha < 3/2$, and perhaps that $\alpha \sim 1$. Thus for a number of storms taken individually, involving dry snow of various crystal types, it may be that k and R are related linearly; however, it is to be expected that a general relationship should show considerable scatter about a linear regression line. These conclusions were confirmed by the experimental results.

Lillesaeter (1965), working from results obtained by Gunn and Marshall (1958) who measured diameters D to which aggregate snowflakes melted (and thus their masses), obtained a set of theoretical values, his Table 2, relating attenuation per unit path length (k), with various rates (R). This table is reproduced in part below:-

R mmw hr^{-1}	0.31	0.70	1.10	2.50
k db km^{-1}	8	13	18	23
$\left(\frac{k \text{ db km}^{-1}}{R \text{ mmw hr}^{-1}}\right)$	26	19	16	9

The omission of diffraction effects from his considerations, Lillesaeter indicates, may have led to overestimation of the ratio k/R.

When these four pairs of values of k and R are plotted on logarithmic paper, a straight line of slope 0.5 fits the points well. That is the attenuation per unit path length is proportional to $R^{0.5}$. This theoretical conclusion differs from the above, and further experimental work as outlined in chapter 5 should be performed.

For wet or rimed snow, the ratio of projected cross section to mass is much smaller than for dry unrimed snow, and the particle fall velocities are higher by a factor of about 2 (Fletcher, 1962,

page 276). Thus the ratio k/R is greatly reduced for wet or rimed snow, and measurements by Lillesaeter and also by the author have confirmed this.

Attenuation by rain

Middleton (1952), on page 122, shows that for rain the extinction coefficient, depending only upon the number (X) of drops falling on 1 cm^2 each second, is given by

$$\sigma_R = 5.2 \quad 10^{-6} \quad (X) \quad cm^{-1}$$

$$= 0.52 \quad (X) \quad km^{-1}$$

This is valid where the particle is of size sufficiently large for the particle scattering area ratio to take the constant value 2. This criterion is satisfied for rain.

Taking X = 1 cm^{-2} sec^{-1} for typical rain, k = 4.34 x 0.52 or about 2 db km^{-1}. Lillesaeter (1965) found attenuations of about 0.25 (db km^{-1})/(mmw hr^{-1}), confirmed by the present author. This value is much smaller than 11 (db km^{-1})/(mmw hr^{-1}), the attenuation encountered in snowfall during the course of this work.

3. Experimental Arrangements

The transmissometer

The transmissometer was set up on the campus of McGill University, between the Otto Maass Chemistry Building and the Macdonald Physics Building (see Fig. 1). The optical path measured 71 ± 0.5 m in length, was about 20 m above the ground and was inclined downwards from the transmitter at $3^{\circ}53'$. The light travelled from SE to NW approximately. The path was high enough to be free of snow drifting from the ground. Snow drifting from the building roofs, and steam from a small chimney on the Chemistry Building, drifted through the beam on occasions, but produced on the recorded trace spikes of short duration, which were easily recognized and ignored in the analyses. Positive identification of occasions of each type are illustrated in Appendix 3.

The optical system is shown in Fig. 2 and is similar to that used by Lillesaeter (1965). The light source was a stroboscope (General Radio Type 1531-A) - fed through a constant voltage transformer - with a xenon arc discharge of dimensions approximately 8 mm x 3 mm. The spectrum covered the visible with a broad maximum centred at about 0.47 μ (see Fig. 20, Appendix 2). The flash duration was 3 μsec and the stroboscope was set to flash at 3.8 cycles sec^{-1} (rather than exactly 4 cycles sec^{-1}, a sub-multiple of the AC mains frequency). A pulsed light source was chosen to eliminate the variable effect of daylight that would have been encountered with the use of an otherwise similar steady light source.

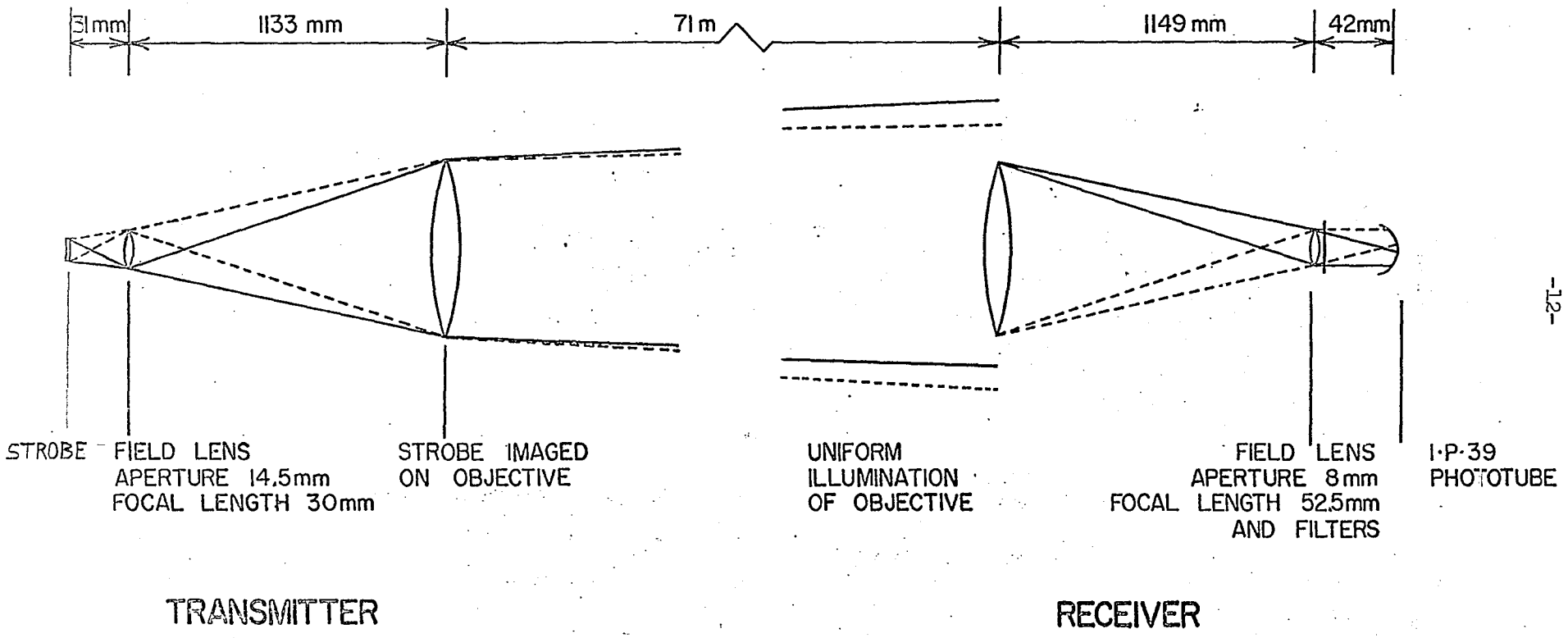

Fig. 2 The optical system

The transmitter consisted of the stroboscope source and a reflecting telescope of mirror aperture 10.4 cm and focal length 1.14 m. (For simplicity a refracting telescope is shown in Fig. 2.) A field lens of aperture 14.5 mm and focal length 30 mm imaged the small dimension (3 mm) of the source near the objective. The geometry was such as to produce a nearly parallel transmitted beam. The location of 14.5 mm diameter field lens established the semi-angle of divergence of the beam at 0.34°. Thus the receiver, of aperture 10.4 cm, intercepted only a small fraction of the transmitted light at the centre of the beam. This arrangement was made so that the signal would not be sensitive to small deflections originating near or at the transmitter, as had been the case with Lillesaeter's experiment where the image of the transmitter field lens nearly matched the receiver aperture.

The receiver, similar to the transmitter, consisted of a reflecting telescope that concentrated the incoming light on to the cathode surface of a vacuum phototube (R.C.A. type 1P39, with S4 response illustrated in Fig. 20). The optical system was such that about 16 mm^2 of the 150 mm^2 semi-cylindrical surface of the photo-cathode was illuminated. The 8 mm aperture of the receiver field lens resulted in a field of view with semi-angle 0.19°. At the transmitter this corresponded to a circle of diameter 50 cm, about 5 times the transmitter aperture. The front surface of the wooden transmitter telescope box was painted flat black to minimize scatter of daylight into the receiver.

Filters were inserted at the receiver field lens, a Kodak Wratten Gelatin filter No. 47 with a peak of transmission at 0.44 μ (Fig. 20), and also Kodak Wratten neutral density filters that were used to adjust the signal level and for calibration purposes (see Appendix 2).

The output from the photocathode was amplified and smoothed, and the signal recorded on two Esterline Angus Model AW strip chart recorders, run normally at 3 in hr^{-1}. On occasions during one or two of the storms they were run at 3 in min^{-1} for periods of 24 mins (see Appendix 3). The circuit (Fig. 21) and further experimental details are described in Appendix 2.

The instruments of McGill Observatory

There were two tipping-bucket gauges, called for convenience "East" and "West" (Department of Transport standard M.S.C. pattern). Insulation and thermostat-controlled heaters had been added. The heating differed for the two gauges, but was designed to maintain the receiving funnel surfaces at a temperature a degree or two above 0°C so as to melt incident snow. The gauges' performance was variable in that the snow accumulations recorded by each differed (see Table 1, chapter 4). This was chiefly because adjustments towards optimum thermostat settings were being made during the winter. That the adjustment was not ideal was evident on at least one occasion when steam was seen rising from a receiving funnel. The heating undoubtedly led to evaporation losses, which were important at low rates of snowfall.

The effects of wind flow on the records of the tipping bucket gauges and the Nipher gauge are not known. As is seen from Fig. 1, the wind shielding was different for the two instruments. The Nipher shield was a solid curved shape, and an Alter shield consisting of a system of slats mounted on a circular frame protected each of the bucket gauges.

From April 1966, a precipitation sensor (No. 598-2, Science Associates Inc.) has been in use at McGill. This was of great value in determining times at which snowfall began. Its performance was rather insensitive to times of cessation owing to residual quantities and blowing snow, and it did not give precise indications of start and finish times in conditions of very light intermittent snowfall.

4. Results and Discussion

The storm of 25th December 1966

Among the snowstorms of the winter of 1966-7, that of 24th - 26th December 1966 has been analysed in detail. This storm deposited at Montreal a total of about 33 mmw over 30½ hours. Moving eastwards slowly the low centre passed close to the city. Storms of such magnitude occur but once or twice during the course of a season, and generally result from the action of a blocking high pressure area located north-eastwards of the precipitation zone, with the Westerlies displaced well south of the normal latitudes (Andrews, 1967).

Routine observations of accumulated precipitation at McGill Observatory are made twice daily at 0900 and 1700 hours. The storm was analysed in three components as follows: 2100 24th Dec - 0900 25th Dec; 0900-1700 25th Dec, and 1700-0330 26th Dec. The chart recorder trace for the first half of the storm, 2100 24th Dec - 0900 25th Dec, in which fell about 23 mmw, is shown in Fig. 3. Attenuation was measured upwards on the paper from the "base line", which represented the signal level for zero snowfall density. It is seen that the attenuation varies markedly during this period, and that a useful comparison may be made between attenuation and rate of snowfall, as indicated by the time separation of tips of the bucket gauge, marked along the bottom edges in Fig. 3. The record of the East tipping bucket gauge was used, as the recorded number of tips corresponded well with the accumulation in the Nipher gauge over the period; the record of the West gauge was erratic. After 0900 25th December both the tipping bucket gauges gave performances which seemed to be

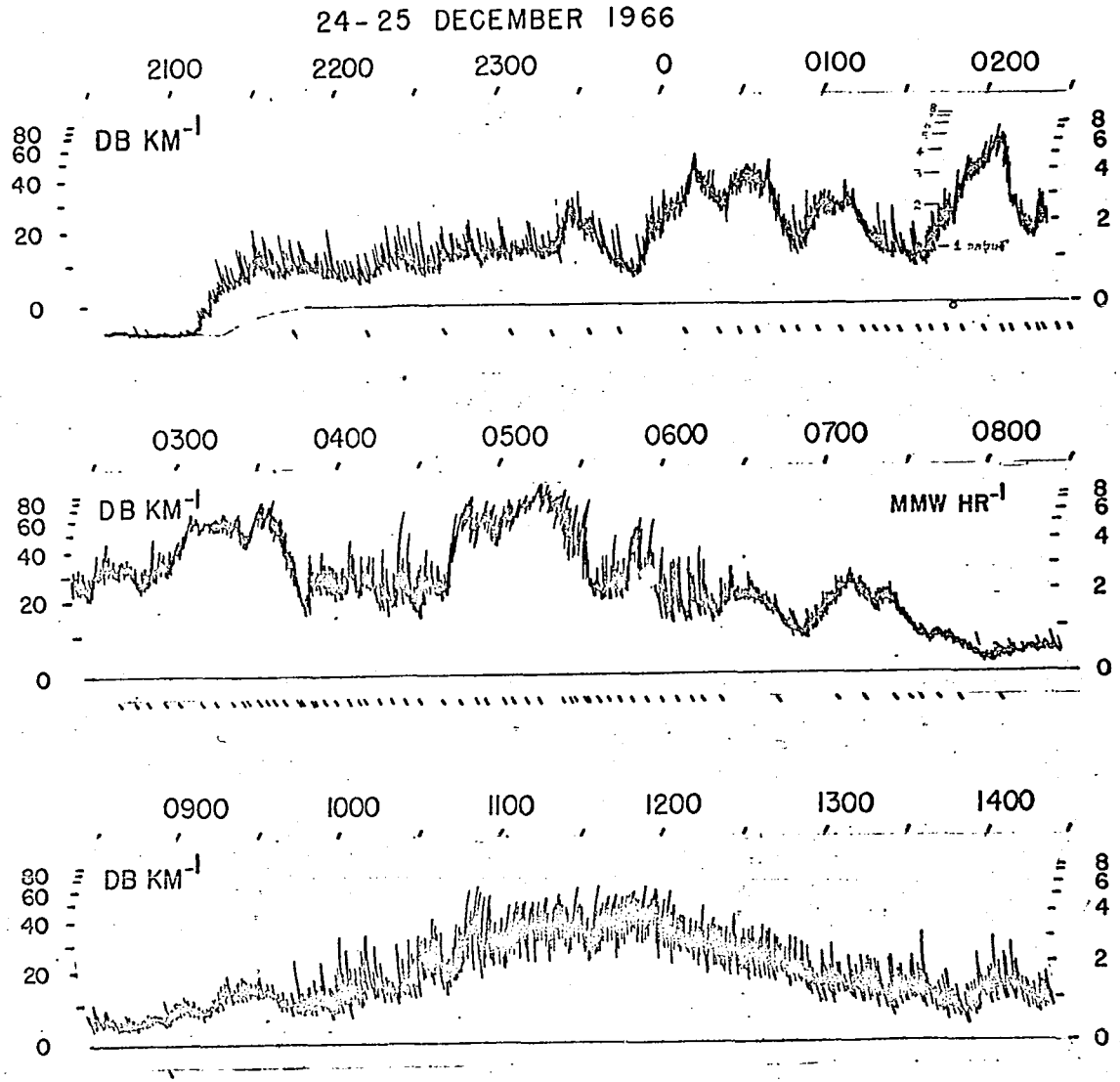

Fig. 3 Chart recording of the first 18 hours of the storm of 24-26th December 1966

not representative of the snowfall, and only the total accumulation of snow during the second half of the storm was considered. The division at 0900 25th December was convenient from a meteorological point of view, because at that time a minimum of snowfall rate occurred and afterwards the prevailing wind shifted from NE 12 mph to W 18 mph, with the low centre at its closest to the Observatory at 1230 hours.

The first step in the analysis was to draw in the base line. Of assistance here was the record of the precipitation sensor, indicating the times of the start and finish of the storm. As discussed in Chapter 2 and Appendix 1, the position of this line is dependent on relative humidity. At the beginning of the storm the relative humidity was 68%, and after an hour of snowfall it was 85%. At the end of the storm it was 85%. The base line was drawn in as a straight line from its position at the end of the storm (90 divisions) backwards in time to 2200 24th December, an hour after the beginning of the storm. The ends at 2100 and 2200 of the base line were then joined together in accordance with the growth of relative humidity between these times from 68% to 85%. This general procedure was followed for all the storms analysed.

Next, the mean attenuations for each consecutive five minute interval were tabulated, using a calibration curve such as that shown in Fig. 22, Appendix 2. From these, the mean attenuations over consecutive half-hour periods were calculated. Correspondingly, the number of bucket tips during the consecutive half hours were tabulated, and rates of precipitation in mmw hr^{-1} obtained. After conversion of

the attenuations from db $(71m)^{-1}$ to db km^{-1} the 24 pairs of values thus obtained were plotted on logarithmic paper (Fig. 4).

This diagram shows a considerable scatter of the points. In examination of this scatter, new diagrams were produced using quarter-hour rather than half-hour intervals, and also allowing for a 10-minute lag in the performance of the tipping bucket gauge. No reduction in the scatter was obtained. Further, a 91 point attenuation-rate scattergram was made for the 91 tips - each representing $\frac{1}{4}$ mmw - of the East gauge over the period. This again showed no improvement.

Fig. 6 is a comparison of accumulations. The 12 hours of the storm period are on the abscissa. The diagram was constructed in two steps. First the mean attenuations (db km^{-1}) over consecutive 5 min intervals were added up to give a running total at any time of accumulated (db km^{-1}) 5 mins. The running total thus represented for any time the area of the chart recorder paper between the base line and the curve traced out up to that time by the chart recorder pen. It was plotted on a convenient ordinate scale, the final accumulation - or total area under the attenuation curve - being represented as the final value of accumulated (db km^{-1}) hr. The slope of the curve thus drawn is at any time a measure of the attenuation at that time.

With this done, the ordinate scale interval obtained was divided into 91 equal parts to correspond with the 91 x $\frac{1}{4}$ mmw accumulated by the East tipping bucket gauge, and each tip number and tip time were used to obtain an accumulation curve of the precipitation recorded by the gauge. The slope at any time of the second curve gives

the rate of precipitation at that time. With perfect correspondence between attenuation and rate of precipitation the two curves would coincide.

It is seen from this curve that disparity exists at low rates at the beginning and end of the storm period, and that there are anomalies at 0645 and 0730. These two occasions are shown up on Fig. 4 by the wide separation of the points designated 0645 and 0745.

The scatter of the points on Fig. 4 is such that it is not justifiable to assign an index other than one to the relation between attenuation and rate. Then assuming linearity the accumulated 22.75 mmw may be divided into the accumulated 291 (db km^{-1}) hr to obtain 12.8 (db km^{-1})/(mmw hr^{-1}), or $k = 12.8\ R^{1.0}$. This linear relationship is drawn as a line of slope 1 in Fig. 4.

Noting the discrepancy at low rates, it is reasonable to make a correction based on an assumption that loss by evaporation occurs from the receiving surface of the tipping bucket gauge. To make a correction, the ratio of (k/R) was tabulated for each half-hour interval, and the minimum value was divided into the maximum value of this ratio to obtain a numerical measure of the extreme of scatter about a linear regression line. Then denoting a constant rate of evaporation by E, various values of E were added to R and the process repeated with tabulations of (k/R+E). Thence was obtained an optimum value of E for a minimum of the extreme of scatter about a linear regression line. This simple process yielded 0.38 mmw hr^{-1} as the evaporation rate. Figs. 5 and 7 show the result of this correction, corresponding with Figs. 4 and 6. It is seen that the accumulation curves correspond

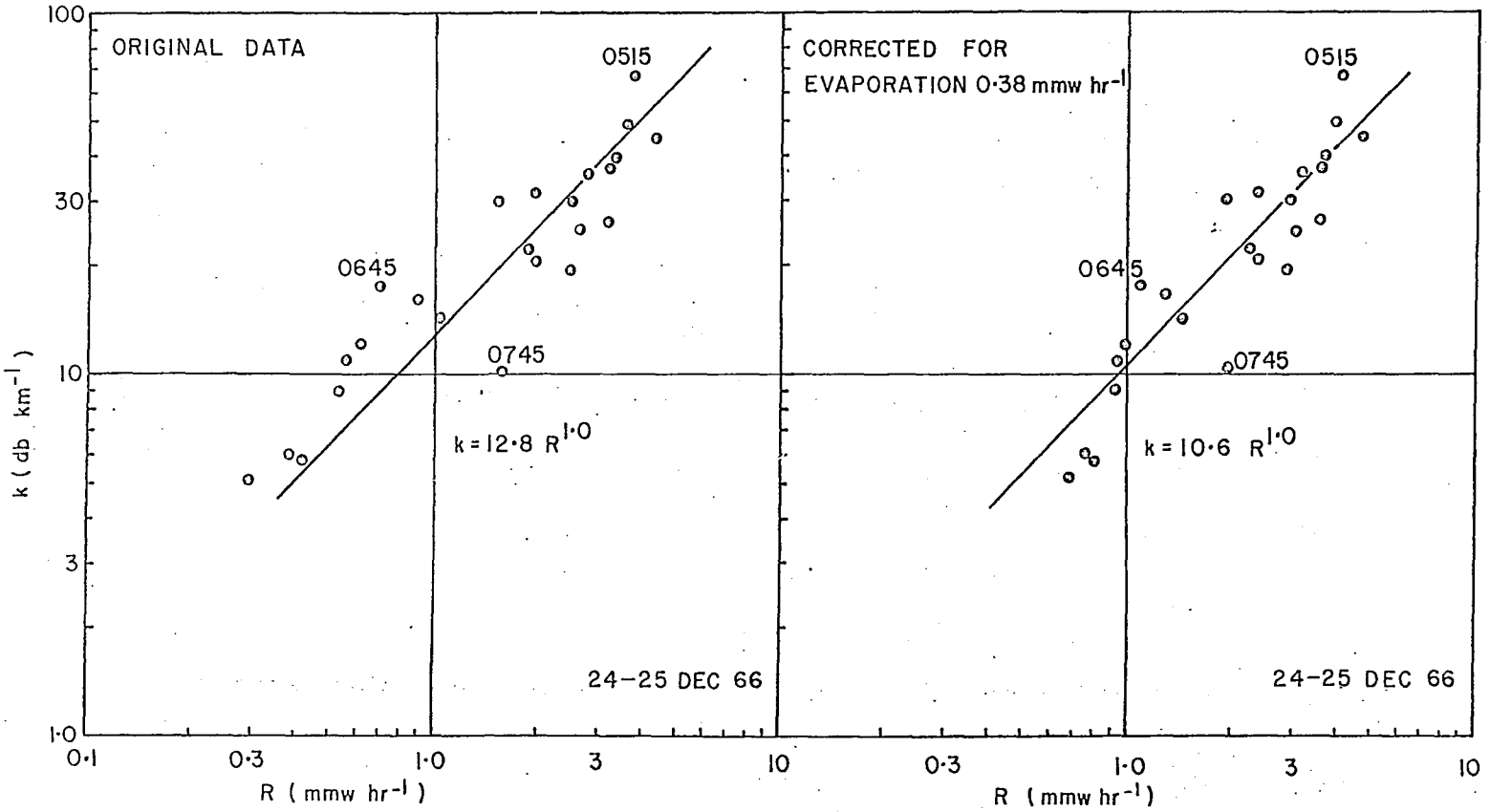
ORIGINAL DATA
0515
0645
0745
k = 12·8 R^1·0
24–25 DEC 66
k (db km^-1)
R (mmw hr^-1)
100
30
10
3
1·0
0·1
0·3
1·0
3
10

Fig. 4

CORRECTED FOR
EVAPORATION 0·38 mmw hr^-1
0515
0645
0745
k = 10·6 R^1·0
24–25 DEC 66
R (mmw hr^-1)
0·3
1·0
3
10

Fig. 5

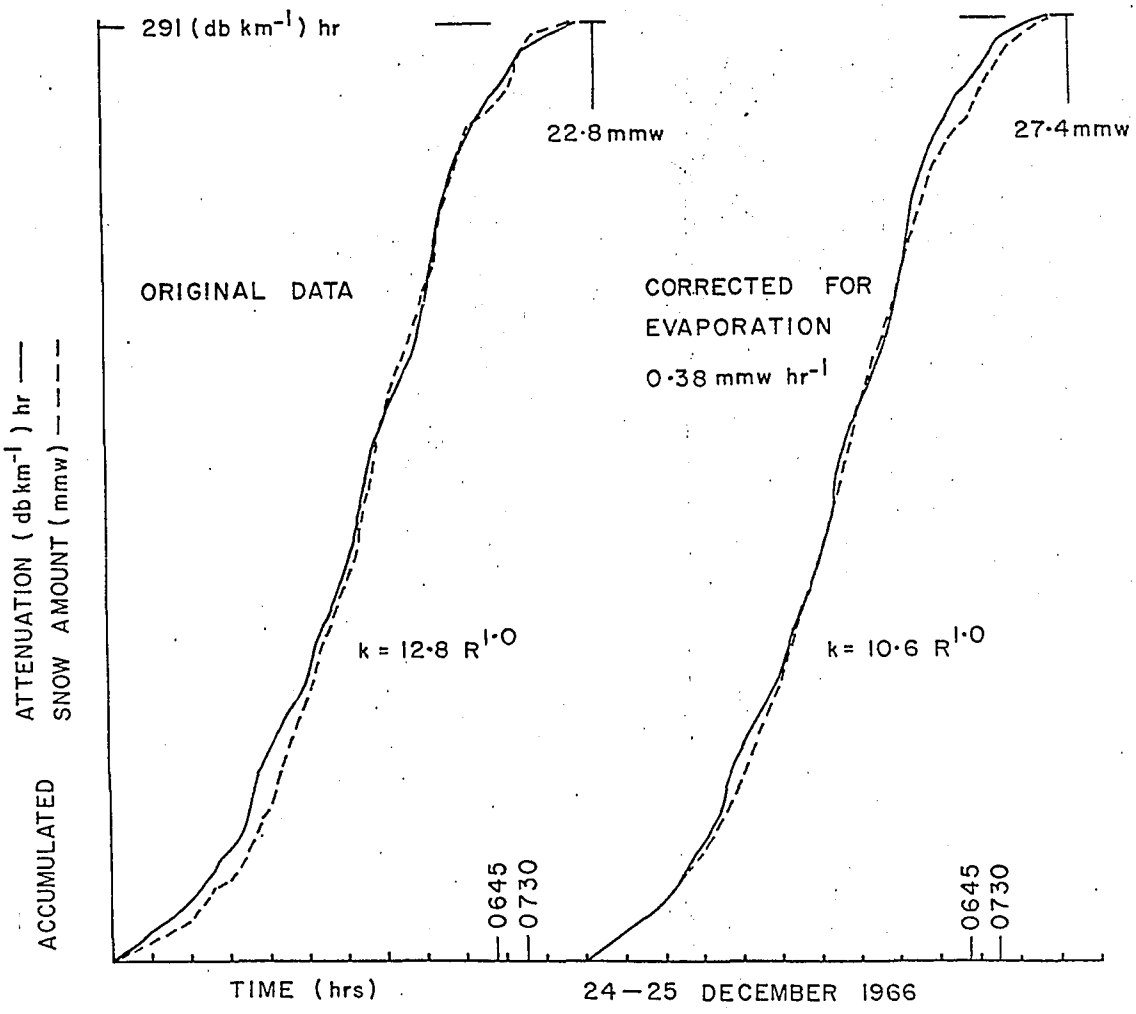
291 (db km⁻¹) hr
22·8 mmw
27·4 mmw
ORIGINAL DATA
CORRECTED FOR EVAPORATION
0·38 mmw hr⁻¹
k = 12·8 R^1·0
k = 10·6 R^1·0
ACCUMULATED ATTENUATION (db km⁻¹) hr ——
SNOW AMOUNT (mmw) – – – –
0645
0730
0645
0730
TIME (hrs)
24–25 DECEMBER 1966

Fig. 6

Fig. 7

much better, but the 0645 and 0730 anomalies remain. These are attributed to erratic behaviour of the gauge. The accumulations now yield the linear relationship $k = 10.6\ R^{1.0}$.

It is reasonable to question the validity of taking the evaporation as constant. To examine the effect of variable evaporation rate, proportionality was assumed between evaporation rate and the product of the mean wind speed over hourly intervals and the vapour density difference between saturation at 273°K and the ambient conditions. The latter quantity (Z) is plotted in convenient units against time in Fig. 8. Denoting the evaporation E mmw hr^{-1} as equal to (x Z), with x a constant, the tabulation procedure as outlined above to obtain the minimum extreme of scatter about a linear regression line was again performed, this time using $(k)/(R + xZ)$ to obtain an optimum value of x. This procedure yielded Figs. 9 and 11, with a mean evaporation rate for the storm period of 0.49 mmw hr^{-1}, reaching a maximum at 2245 of 0.63 mmw hr^{-1}. It is seen that the scatter of points in Fig. 9 shows no improvement, and the accumulation curves show a poorer correspondence than does Fig. 7. The linear relation for this case was $k = 10.1\ R^{1.0}$. The lack of improvement in the accumulation diagram, together with the high evaporation rates obtained, suggested that perhaps the assumption of a constant evaporation rate was best. Similar analysis of the two other major storms of the season, those of 29 December and 27th - 28th January confirmed this conclusion.

The evaporation correction made a small difference to the slope of the lines of best fit through the points in Figs. 4, 5 and 9. With no evaporation this line had slope slightly less than 1; with

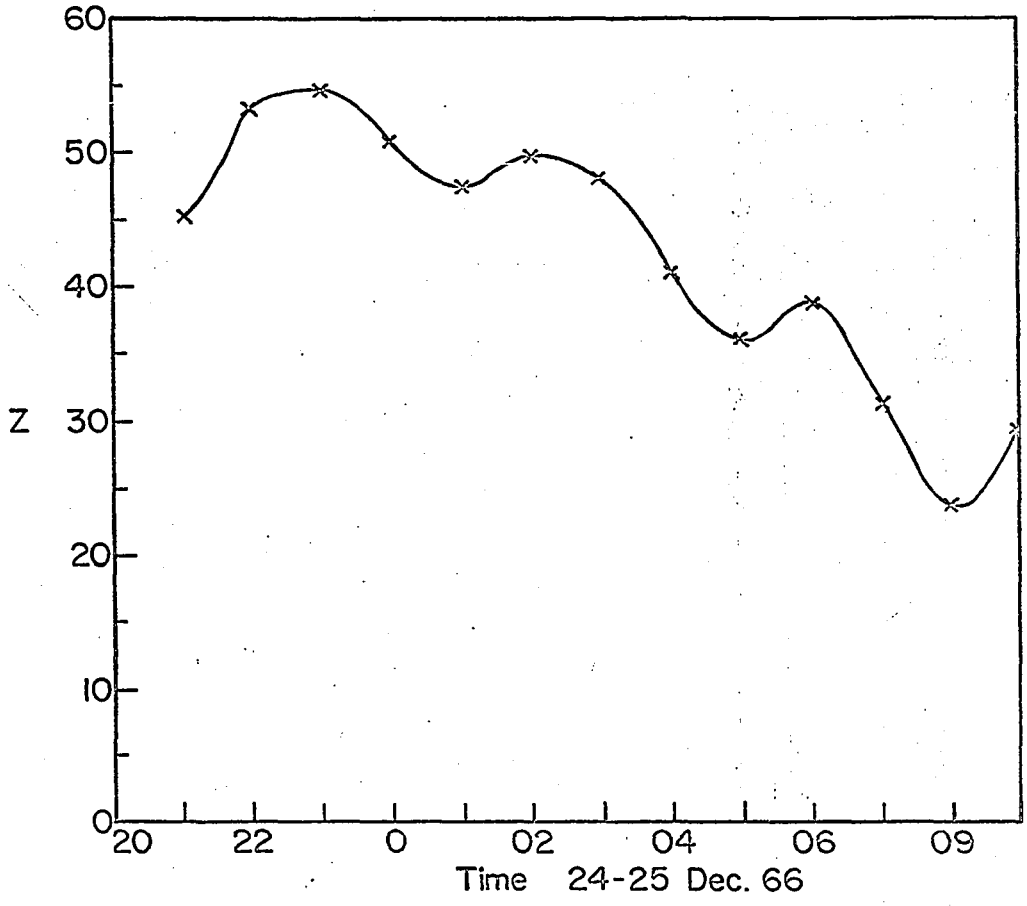

Fig. 8 Variation of the tendency for evaporation (Z)

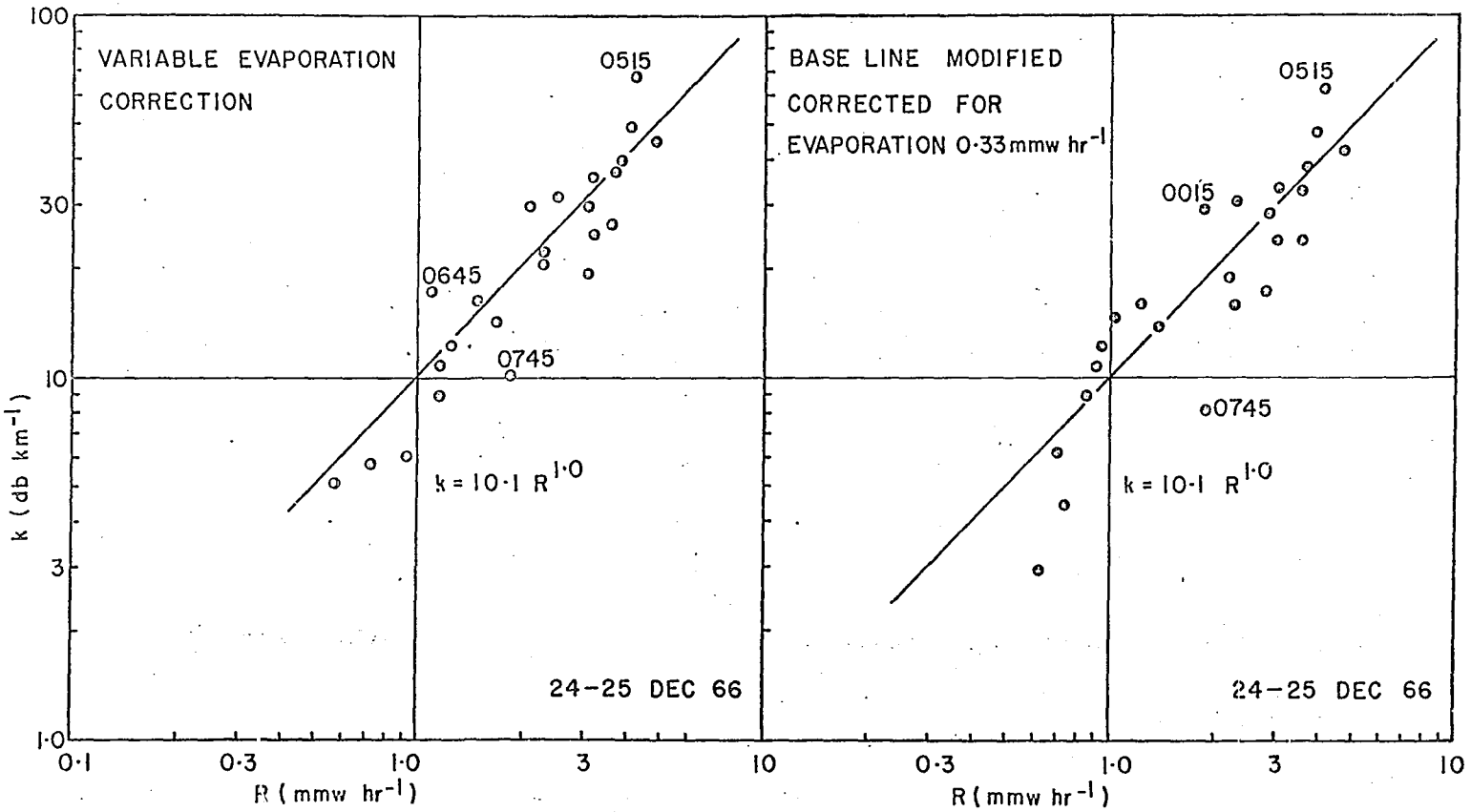
VARIABLE EVAPORATION
CORRECTION
0515
0645
0745
k = 10·1 R^1·0
24–25 DEC 66
k (db km⁻¹)
R (mmw hr⁻¹)
100
30
10
3
1·0
0·1
0·3
1·0
3
10

Fig. 9

BASE LINE MODIFIED
CORRECTED FOR
EVAPORATION 0·33mmw hr⁻¹
0515
0015
0745
k = 10·1 R^1·0
24–25 DEC 66
R (mmw hr⁻¹)
0·3
1·0
3
10

Fig. 10

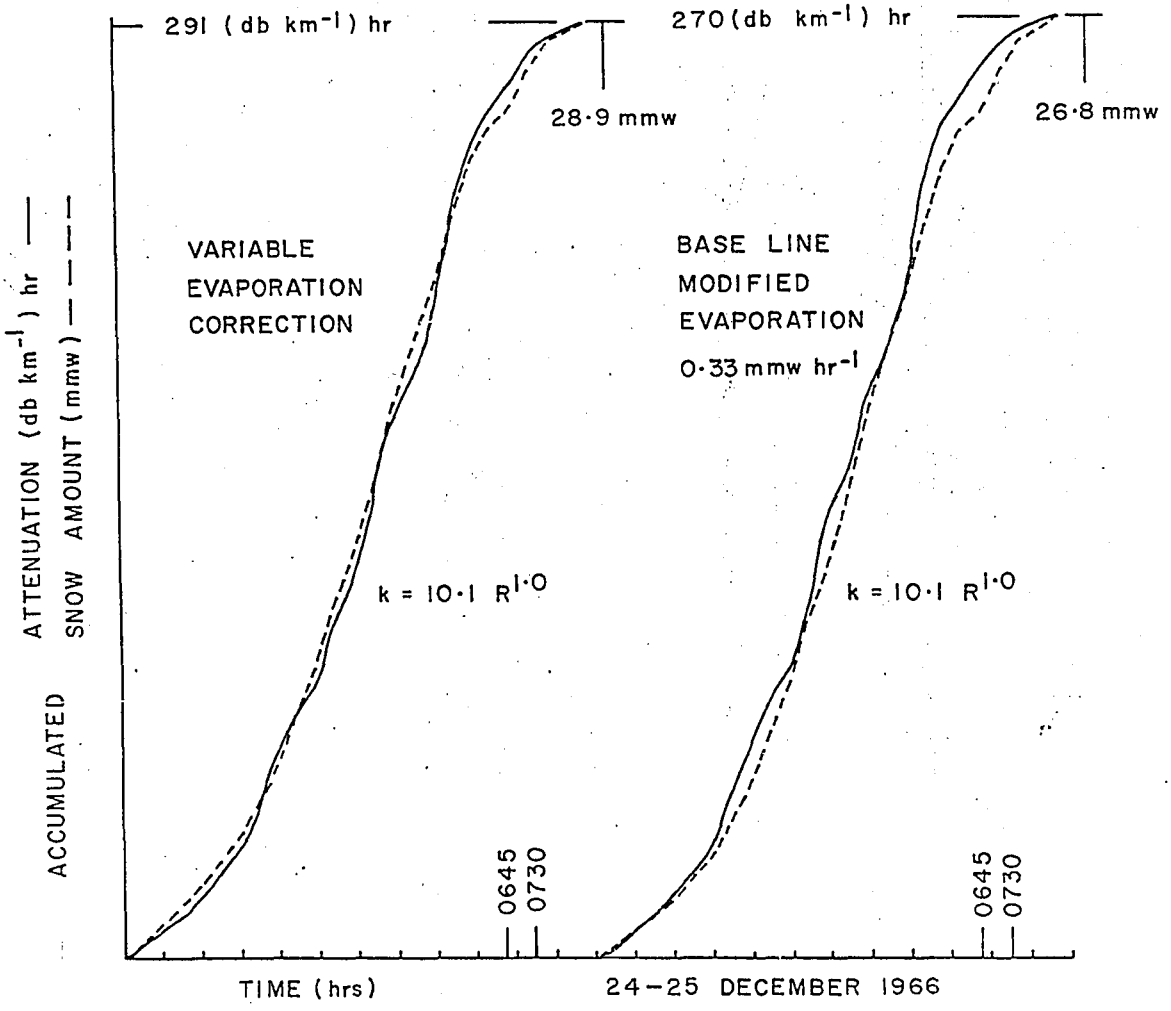
291 (db km⁻¹) hr
28·9 mmw
VARIABLE
EVAPORATION
CORRECTION
k = 10·1 R^1·0
0645
0730
270 (db km⁻¹) hr
26·8 mmw
BASE LINE
MODIFIED
EVAPORATION
0·33 mmw hr⁻¹
k = 10·1 R^1·0
0645
0730
ACCUMULATED ATTENUATION (db km⁻¹) hr ——
SNOW AMOUNT (mmw) — — — —
TIME (hrs)
24–25 DECEMBER 1966

Fig. 11

Fig. 12

the evaporation correction the slope became slightly greater than 1. However, the differences from slope 1 in all cases were small.

Finally it was necessary to examine the effect of possible changes in position of the base line as this depended upon the presence of a haze generated by the snowfall. As a first approximation the component of the attenuation of the light due to this haze was modelled on the basis of relative humidity measurements made with the instruments of the McGill Observatory. Fig. 19, Appendix 1, page 51, represents typical changes of attenuation in "clear air" with changes of relative humidity. Taking the solid line labelled 25 Dec 1966 as representative of the storm period under consideration, an adjustment was applied additively to the half-hour mean values of attenuation (k) in db km^{-1}. This adjustment was zero at 85% relative humidity, and the amount to be subtracted rose as the relative humidity rose above the 85% level during the storm. Thus from a tabulation of relative humidity at half-hour intervals a set of adjusted values of k was obtained. A scattergram and an accumulation diagram were obtained for which an optimum constant evaporation rate was found to be 0.33 mmw hr^{-1}. These are Figs. 10 and 12. The accumulation diagram showed poor correspondence between the two curves, and yielded for a linear relationship $k = 10.1\ R^{1.0}$. From the scattergram it is seen that the line of best fit would have slope greater than 1. This was due to the marked effect that both the relative humidity adjustment and the application of the constant evaporation rate had on the low value points.

A relation between attenuation and rate of snowfall

From the analysis of the storm of 25th December it is possible to say only that the relation between attenuation (k db km^{-1}) and rate (R mmw hr^{-1}) is approximately linear. The constant of proportionality between k and R was sensitive to the correction for evaporation, changing the value of 12.8 for the original data, to 10.6. Similar changes were found in detailed analyses of other storms. For all the winters' storms the value of 11.0 was chosen as being reasonable and representative, and the relation $k = 11.0\ R^{1.0}$ was used to calculate accumulations of mmw for most of the storms which were compared with the raw data taken at McGill Observatory. These results are presented in the next section, and the good agreements obtained give confidence that $k = 11.0\ R^{1.0}$ is a reasonable average relation to use throughout a season.

Regarding scatter of the points on the plots of k against R for 25th December, it is notable that the scatter remained but little affected by the evaporation correction, and that the degree of scatter was not sensitive to small changes in the value assumed for the evaporation rate. The rather crude method used to determine the optimum was dominated by the three points representing 0745, 0645 and 0515, which gave the extremes of scatter.

Figure 13 is to show how the scatter of points obtained from the storm of 25th December (Fig. 4) corresponds with that of points similarly obtained from the other major storms of the season. The data are unmodified; there is no evaporation correction involved in this diagram. Six storms are represented, which deposited about 83 mmw

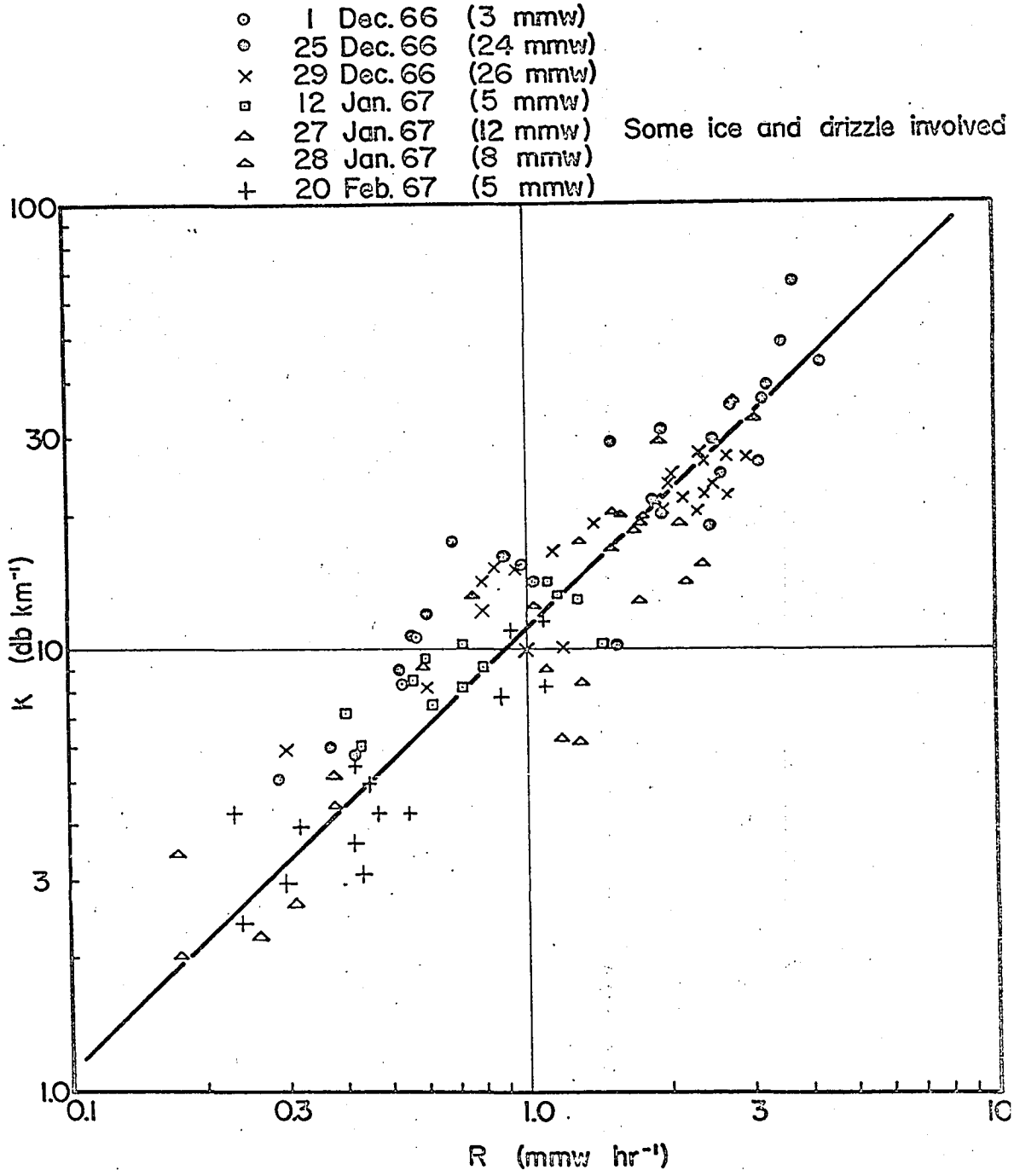

Fig. 13 Scattergram for the major storms, 1966-7

over about 50 hours. The scatter is similar for all the days, and the points are grouped about a line of slope 1. All but 3 of the approximately 100 points lie within a factor ±2 of the relation $k = 11.0\ R^{1.0}$, and about 75 of the hundred lie within a factor ±1.5.

The snowfall of the winter 1966-67

Table 1 displays information on most of the winter's snowfall, 160 mmw which fell over a total period of 200 hours. The remaining 36 mmw, which fell over 151 hours, are not treated, principally because of the low rates, very small attenuations, involved; there was one occasion involving 5.75 mmw falling over a 10-hour period on which the transmissometer was malfunctioning. It was difficult to obtain valuable results on snow falling at low rates of accumulation because of the sensitivity of the measured attenuations to positioning of the base line.

Column 3 of Table 1 shows the calculated values of accumulated (db $(7\text{km})^{-1}$ 5 mins) over each storm of date shown in column 1. With $k = 11\ R^{1.0}$ it is possible to calculate amounts of accumulated water. In units of inches of melted-water these amounts appear in column 4. The conversion factor was 0.00420. The units (inches of melted water) are used for direct comparison with the values read at McGill Observatory from the gauges, columns 5 to 9. Columns 6 and 8 refer to the numbers of tips of respectively the "East" and "West" tipping bucket gauges, and columns 5 and 7 to the water catches in the containers beneath the buckets of these gauges. Column 9 represents the melted catch of the simple unheated open Nipher gauge can. Each

Date	Duration hours	Accum'd $db(7lm)^{-1}$ 5 mins	Amount from $k=1.0$ 11 R	McGill Observatory — Inches of water — E can	E tips	W can	W tips	Nipher	New Snow Inches	Wind Maxima	Notes
1.12	7.75	39.5	.17	.10	.07	.09	.07	.11	1.7	NW 6	
25.12	12	252	1.08		.91	.91	.63	.95	10	NE 15	
	8	125	.53		.11		.12	.24	4.5	W 20	
	10.58	83	.35			.12		.13	.9	W 20	
29.12	15.83	211	.90	.92		.89	.88	1.05	10	S 10	
	6.75	31	.13			.03	.03	.08	1	W 9	
7.1	3.75	36	.15		.16	.18	.14	.21	1.5	NE 9	Some ice or rain
12.1	10.5	51.5	.22		.13	.14	.12	.20	3.2	SW 10	
17.1	3.17	14.5	.06		.04	.07	.04	.06	.7	SW 7	
27.1	18.17	182	.78	.75	.73	.84	.97	1.09	5.5	NE 13	Some ice + drizzle
28.1	6.33		.37		.29		.38			NE 14	
4.2	8.5	49	.21	.08	.07	.11	.12	.16	1.8	SW 7	
11.2	3.33	26	.11		.03		.02	.05		SW 14 and NW 14	
15.2	16.67	75	.32	.42	.46	.40	.47	.69	2.5	NE 13	Mixed pptn.
20.2	14.33	61	.26	.21	.20	.22	.25	.38	3.0	NE 11	
27.2	21	128	.55	.21	.23	.27	.28	.42	3.8	SW 7 and NW 10	
5.3	8	11	.05	.02	.03	.03	.03	.07		NE 6	
13.3	9.5	75	.32	.16	.17	.155	.16	.23		SW 5	Mixed pptn.
19.3	6.33	11	.05					.03		W 10	
21.3	11.33	57	.24	.05	.05	.06	.05	.15	2.0	S 11	
7.4	4.58	14	.06	.04	.03	.06	.06	.07		NE 10	
			6.91"					6.37"			

TABLE 1.

column shows accumulations reported to the nearest hundredth of an inch. With the instruments performing perfectly, all the values of columns 5 to 9 would read the same amount on any one occasion. It is seen that the instrumentation is not perfect, that there must be considerable doubt as to total accumulations. The Nipher gauge accumulation is in nearly all cases greater than the other amounts reported. Column 10 is a record of new snow that accumulated on a 10 cm x 10 cm plastic marker placed on the old snow surface at a site near that of the other instruments. This depth was measured by inserting a thin plastic ruler and reading to the nearest tenth of an inch.

Figs. 14 and 15 show logarithmic plots of values of calculated amounts per storm using $k = 11.0\ R^{1.0}$ (column 4) versus amounts in the Nipher gauge (column 9), and new snow depth (column 10) respectively. These figures give an indication of how useful the transmissometer may be in evaluating total snowfall quantities. In general, the analyses followed the procedure outlined in the description for the storm of 25th December - the second and third periods of this storm as well as the first being here included.

Fig. 14, a comparison of values calculated according to the relation $k = 11\ R^{1.0}$ with Nipher gauge accumulations represents 150 mmw of melted snow. Slightly more than half the points lie above the one to one relationship line. This indicates that either the attenuation measurements were giving values that were too high, or that the Nipher gauge tended to collect too little. The first part of the 25th December storm yielded the largest calculated accumulation and the point representing it lies close to the one to one line. The second

and third parts of the 25th December storm yielded points outside a factor two limit, and so did the storm of 11th February. In the former case the wind was very strong (18 mph) and from the west. In all other cases the wind was either from the east or northeast, or was light if from the west or southwest. It is reasoned that the anomalous points from 25th December result either from a reduced catch in the gauges, or to re-circulating snow from ground or roof surfaces resulting in anomalously high attenuations. The chart recorder trace showed considerable high frequency variations in the later periods of the 25th December storm; this lends support to the latter conclusion. The storm of 11th February was especially short and intermittent, with a narrow peak of attenuation reaching a maximum of 8.5 db occurring over a period of about ten minutes. The calculated accumulation probably is not more than 15% in error; perhaps the different locations of the optical path and the gauges were of importance here, though the horizontal distance was only about 50 m.

Fig. 15 is the comparison between accumulations calculated on the basis of $k = 11\ R^{1.0}$ and the estimates of new snow measured from the plastic marker (expressed in cm). The depth estimates were available for only 15 of the 20 storm periods, those shown by solid symbols on Fig. 14. 130 cm or 4 feet of snow are represented.

The points are grouped much more closely about the one to one line. Only one point lies outside the factor ± 1.5 limits: that for the third part of the 25th December storm is probably in error due to snow being blown away from the measuring marker.

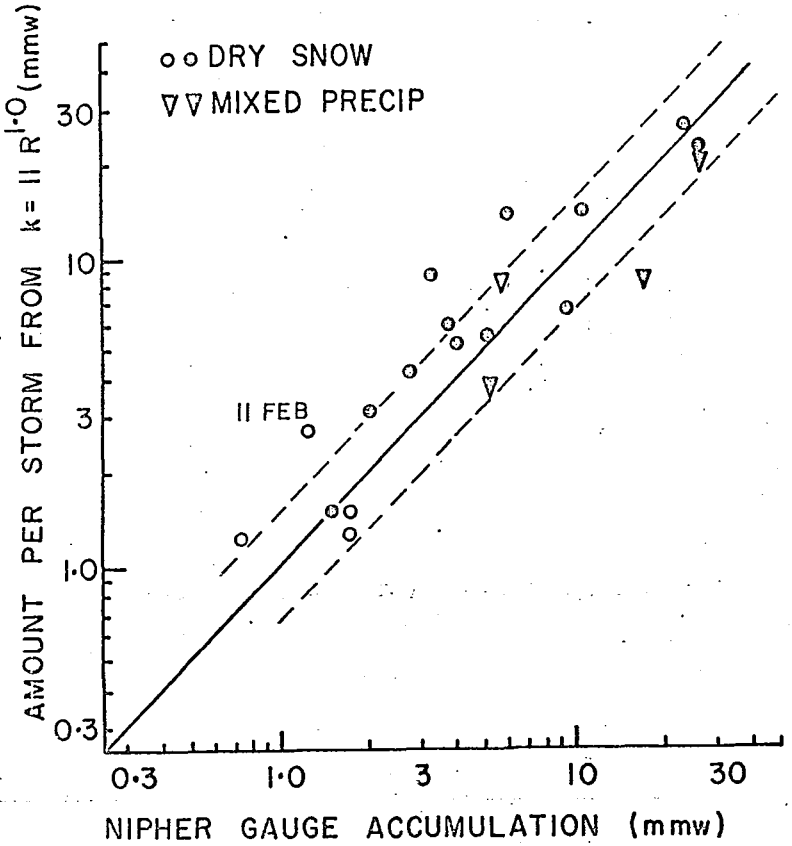
o o DRY SNOW
▽▽ MIXED PRECIP
11 FEB
AMOUNT PER STORM FROM k = 11 R^1·0 (mmw)
0·3
1·0
3
10
30
NIPHER GAUGE ACCUMULATION (mmw)

Fig. 14

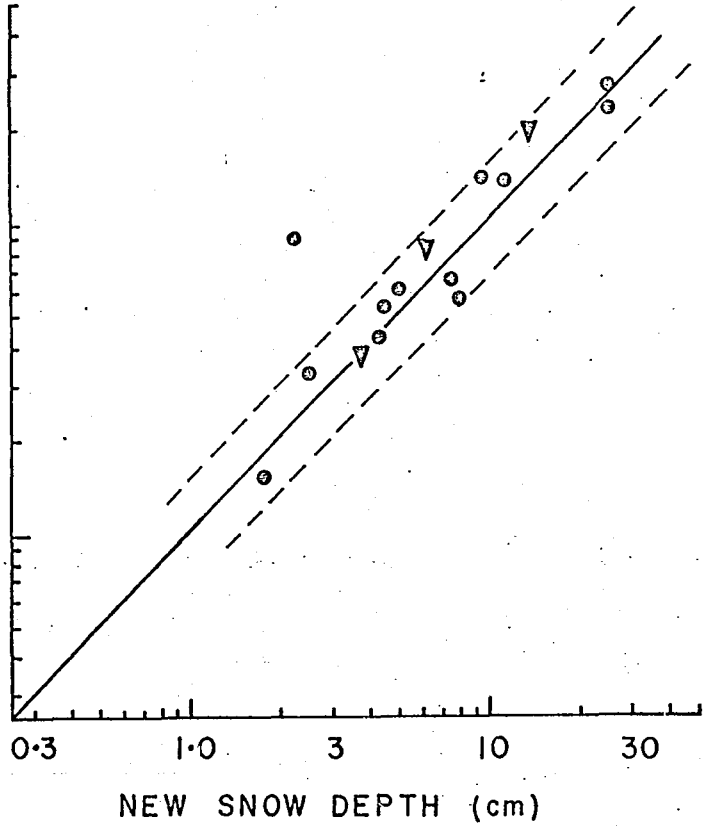
0·3
1·0
3
10
30
NEW SNOW DEPTH (cm)

Fig. 15

Involved in four of the storms were small quantities of ice pellets or freezing drizzle. These storms are represented by triangles. The ice or rain had little effect on the attenuation and the depth of snow on the ground, but did contribute significantly to the total accumulated in the Nipher gauge.

It is interesting to note that the correspondence between the calculated accumulations and the depths of new snow is significantly better than when the Nipher gauge accumulation of melted water is compared. Here is evidence of the importance of crystal type. It may be concluded that there is response in the optical link both to the quantity of water that a snowfall represents, and to the crystal type of the snow. The greater degree of scatter in Fig. 14 as opposed to Fig. 15 can be attributed to variations in density from storm to storm, the storms with snow of lower than average density tending to lie above this line, and of higher than average density below. Large aggregate crystals which pack on the ground at a low density give relatively large attenuation per unit mass compared with small single crystals which pack with higher densities.

Beam Geometry

As described in the previous section, an average relation between attenuation and snowfall rate was found to be $k = 11.0\ R^{1.0}$. Lillesaeter (1965), working with similar equipment, obtained the relation $k = 18.0\ R^{1.0}$. This was based on 10 storms involving a total of 27.5 mmw. Fig. 14 is based on 20 storm periods involving about 160 mmw as accumulated in the Nipher gauge.

Apart from the difference in path length, 123 m as opposed to 71 m, the only other major difference was in the beam geometry. Using the section shown in Fig. 16, the beam volume may be calculated as follows.

Let L be the path length, D be the aperture, the same at transmitter and receiver, α and β be the semi-angles of divergence of the transmitted beam and the receiver field of view respectively, and (D + 2t) be the maximum diameter of the sampled volume, as shown. Let V_B be the volume of the cylindrical beam, and V_C be that of the excess volume defined on the outside by the conical surfaces of the transmitted beam and receiver field of view. Particles within volume V_B contribute only to attenuation of the light; particles within volume V_C on the other hand are positioned such that scattering of light towards the receiver is possible, so that attenuation is diminished.

It may be shown that

$$V_B + V_C = 1/3 \cdot \pi/4 \cdot 1/2\,(1/\alpha + 1/\beta)\,\left[(D + 2t)^3 - D^3\right],$$

$$= 1/3 \cdot \pi/4 \cdot 1/2\,(1/\alpha + 1/\beta)\,2t(3D^2 + 6Dt + 4t^2)\ ;$$

and that

$$V_B = \pi/4\,(1/\alpha + 1/\beta)\,tD^2.$$

Thus

$$\frac{V_C}{V_B} = 2\left(\frac{t}{D}\right) + \frac{4}{3}\left(\frac{t}{D}\right)^2 .$$

t is given by

$$L = t\,(1/\alpha + 1/\beta)$$

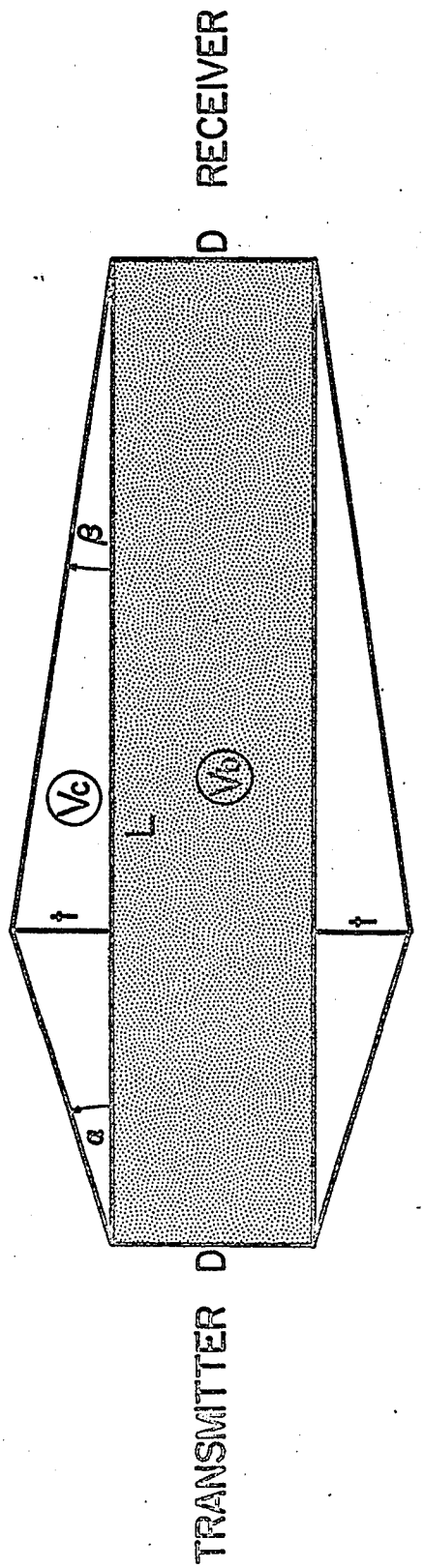

Fig. 16 Beam geometry

and so V_B and V_C are calculated easily.

In Lillesaeter's case L = 123 m, $\alpha = 0.05^\circ$, $\beta = 0.25^\circ$ and D = 10.4 cms. With t = 9.0 cms $V_B = 1.0$ m^3 and $V_C \sim 2.8$ m^3.

In the present case L = 71 m, $\alpha = 0.37^\circ$, $\beta = 0.19^\circ$ and D = 10.4 cms. With t = 15.5 cms $V_B = 0.6$ m^3 and $V_C \sim 3.5$ m^3.

(In the case of the transmissometer at Dorval, considered in Appendix 4, L = 185 m, $\alpha \sim 45^\circ$ ($1/\alpha \sim 0$), $\beta \sim 0.065^\circ$ and at the maximum D = 10.2 cm. This gives that $V_B \sim 1.5$ m^3 and $V_C \sim 14$ m^3.)

The chief difference between Lillesaeter's and the present arrangement lay in the difference between the path lengths and thus V_B. Scattering into the receiver from snow within the volumes V_C probably was of similar magnitude in the two cases. The agreement between the present transmissometer and that of Dorval was good (see Appendix 4) and the Dorval instrument sampling volume V_B was larger than that of Lillesaeter's arrangement. Lillesaeter (1965a) reported an effect of thermal eddies on his narrow transmitted beam, amounting to a loss of the order of 4 db km^{-1} in the most unfavourable circumstances (see his Appendix A1), and this effect might have been responsible for the higher attenuations that he obtained on snowstorm occasions.

To examine the possibility of scattering of light by snow into the receiver, movies of the light source as seen from the receiver were made in various circumstances: in clear air, in smoggy air, and when light powder snow was falling at about 1 mmw hr^{-1}. The camera was held in the same position on each occasion within and near the periphery of the light beam. Several 3-μ sec flashes were recorded on

a number of frames of the film. These frames did not differ significantly in the distributions of recorded light intensity, and it is concluded tentatively that positive contributions of light scattered by snow are not important.

Experimental errors in analysis of the transmissometer records

The possible systematic error in positioning of the base line, or the zero error, considered in the analysis of the storm period of 24-25th December in chapter 4, may be stated as approximately between -4 and +2 db km^{-1}, leading more probably to overestimation than underestimation. This error is poorly known and may have varied systematically in many of the storms analysed. It was always zero at the beginnings and ends of storm periods.

The process of calibration, of deriving and reading calibration curves such as Fig. 22, led to uncertainties of approximately ±6% for all attenuations; the uncertainty of reading the recorded signal from the chart paper was about ±5%. (The inherent noise in the signal, with adjustment for the 71 m path length, amounted to approximately ±0.3 db km^{-1} in normal conditions).

Error due to smoke plumes drifting across the path, and intermittent blowing snow, which produced spikes of high attenuation on the recorded trace (see Appendix 3) were not thought to be significant. Error due to an appreciable time constant of the response of the instrument will arise only if sharp pulses of increased or reduced snowfall rate, superimposed on a steady condition, occur with an assymetry between the rate of growth and the rate of decay. For instance snowfall occurring with pulses of high rate having a sharp

rise in time and a slow decay will be under-read by the optical apparatus if it has a slow response. On the other hand a very fast response would lead to a very noisy trace with a greater reading error. In this case error incurred as a result of the approximately 10-second response time constant was ignored.

The possible random error thus amounted to ±11%. This means that the scatter in plots such as Fig. 4 of attenuation against rate is due not only to errors in measuring attenuations. The scatter should be attributed chiefly to the tipping bucket gauge operation. A time interval was necessary for melting incoming snow, leading to a (variable) time lag of the gauge's operation; this was almost certainly important, though a simple correction for the effect did not reduce the scatter. A part of the scatter must be due to variations in the nature of the snow.

5. Conclusions

Attenuation of a beam of light can provide a useful continuous record of falling snow, with much better time resolution than is available with any standard snowfall measuring device such as a tipping bucket gauge. It can provide data on rates even when the wind is such as to make surface measurements unreliable.

Attenuation appears to be proportional to snowfall rate though the scatter in the rates used for calibration, which came from a heated tipping bucket gauge, was such that a departure from proportionality could not have been detected.

The constant of proportionality was found to be 11 so that the attenuation in db/km was given by $k = 11\ R^{1.0}$ where R is in mmw hr^{-1}. Lillesaeter (1965) found a value 18 rather than 11 for this constant. His higher value can be explained in large part by the effect of thermal fluctuations on his narrow transmitted beam.

The relation $k = 11\ R^{1.0}$ provides good estimates of the total depth per storm of snow on the ground. For 12 storms comprising 130 cms of snow, the estimated depths all lay within $\pm$ a factor 1.5 of the measured depth.

The choice of a path length of 71 m yielded a maximum attenuation due to snowfall of 8.5 db on 11th February 1967: this was equivalent to 120 db km^{-1} or nearly 11 mmw hr^{-1} occurring over a period of less than a minute. A greater path length would have meant greater attenuation for a given snowfall rate, and an unsatisfactory imprecision in measuring high rates, with the existing dynamic range. The calibration characteristic was such as to give increasingly better

resolution at the lower rates, which predominate: 50% of all hours of snowfall at Montreal involve rates less than 0.38 mmw hr^{-1} (equivalent to about 4.2 db km^{-1}) and 20% of all hours involve rates less than 0.1 mmw hr^{-1} (1.1 db km^{-1}) (Gunn, 1965). Half of the total snow amount appears at rates less than 1.2 mmw hr^{-1} (13.2 db km^{-1}).

There was a disturbing effect of the flow of wind around the tipping bucket gauges and the Nipher gauge on the ground. The Nipher gauge consistently recorded greater accumulations than the bucket gauges. This can be accounted for by the evaporation from the receiving surfaces of the latter, were heated to melt the incoming snow. The rates of evaporation, indirectly estimated to be of the order of 0.3 mmw hr^{-1}, probably were as inconsistent as the wind. In addition to this, probably there was an effect of the flow of wind around the structures of the gauges on the areal distribution of the snowfall around the gauge apertures. The Nipher shield was thought to be inferior to the slat (Alter) shielding around the bucket gauges (Fig. 1).

It is possible that correlations could be found between for instance noise on the recorded trace and mean wind speeds and between the variability of rate in time and the prevailing wind vector, among other possibilities, but such effects have not been investigated.

Greatest difficulty in the analyses arose from variations of the signal with relative humidity. Besides the likely imprecision in measuring attenuation, it was necessary to wait until snowing stopped before measurements could be made, so that a base line, or zero attenuation datum, could be drawn in. Perhaps a rearrangement towards a dominant wavelength of 0.75 μ corresponding to the S1 response

characteristic of a photo-emissive tube would reduce these problems. It is at radii of about 0.5 μ and greater that solution droplets would begin to scatter strongly at this wavelength. As the relative humidity passes the critical 80% level the increase in the number of droplets present in the air at this size, and thus the increase in light scattering, might not be very great. Among the hygroscopic nuclei, only those of masses of the order of $10^{-12.7}$ grams could be involved, (see Fig. 17, Appendix 1) and such large nuclei probably are relatively rare. The emission of the General Radio stroboscope intermittent light source (see Fig. 20) used in the present work might be sufficient at 0.75 μ for operation with the existing optical arrangement. With a tungsten lamp and a dominant wavelength in the infra-red, which would be best, probably there would be problems due to heating. The latter possibility was rejected in the present work, when the transmitter design was under consideration, on the grounds of difficulty in obtaining a nearly parallel beam without gross heating effects.

Authoritative work on attenuation of light in haze and fogs is discussed by Arnulf et al (1957) and Eldridge (1966), as mentioned in chapter 2. Eldridge quotes an empirical formula relating visual range (V) km and liquid water content (w) gm m^{-3}, the latter computed from the drop-size distribution in the radius range 0.3 to 10 μ. This relation is $V = 0.024\ w^{-0.65}$. If a simple method could be devised for obtaining values of w during the course of a snowstorm it might be possible to introduce a useful method of correcting for snow-induced haze.

With the optical instrument described in this report, an evaluation of a critical sampling volume might be obtained by varying the transmitter and receiver apertures. The time constant of the response could be adjusted also, though this was thought to be well chosen from the point of view of signal noise during the season of measurement.

It is conceivable that valuable information could be derived from adjustment of the position and orientation of the receiver.

The time involved in maintaining the transmissometer in continuous operation amounted to several hours per week. This was spent chiefly in weekly calibrations and in testing and replacing electronic components when the trace exhibited excessive noise or other peculiarities. The stroboscope bulb was changed three times during the season of measurement, with accompanying changes of permanent filters at the receiver. The optical alignment remained satisfactory throughout the period of measurement, no change being detected. It was necessary to recharge the chart recorders with paper and ink at intervals of about ten days.

One final suggestion is made towards a more sophisticated system: a comparative method might be used, in which the photocell would "see" light coming alternately from the source directly, and from the path. The transmitter and receiver would be one unit, and the remote end of the path would be defined by a three-cornered mirror. The effects of browning over of the stroboscope bulb, and more important the change in characteristics of the amplifier tubes, then would be eliminated. The problem of attenuation due to haze would be unaffected by such redesign, however, and the greater complexity probably would introduce new disadvantages.

Appendix 1. Attenuation in "clear air"

Theory of atmospheric solution droplets

Mason (1962), P20, Eq. 2.2, quotes a formula for the description of equilibrium conditions for a solution droplet of radius (r) involving a nucleus mass (m) of dissolved salt of molecular weight (M_1). With an atmosphere of relative humidity (R H)%, assuming validity of Raoult's Law, the condition for equilibrium of the droplet is given by:-

$$\frac{R\,H}{100} = \exp\left(\frac{2\gamma M}{\rho_L R T r}\right) \quad x \quad \left(1 - \frac{8.6\ m}{M_1 r^3}\right) \qquad (5)$$

where M is the molecular weight of water, ρ_L is the density of water, γ is the surface tension at temperature T°K and R is the universal gas constant. Taking T = 273°K, and expressing m logarithmically as 10^{-n} grams, equation (5) may be reduced to

$$R\,H = 100\ \exp\left(\frac{1.20\ 10^{-3}}{r}\right) \quad x \quad \left(1 - \frac{8.6}{M_1 r^3}\ 10^{12-n}\right) \qquad (6)$$

where (r) is in microns.

The limiting nucleus mass (n′) of salt of solubility (p) grams per 100 cc. of water at T = 273°K, capable of forming at saturation a solution droplet of radius (r)μ, is given by:-

$$\frac{4\pi r^3\ .\ 10^{-12}}{3\ .\ 100} = \frac{10^{-n'}}{p} \qquad (7)$$

or

$$(14 - n') = \log_{10} 4.2p \div 3 \log_{10} r$$

Fig. 17 illustrates the equilibrium conditions for solution droplets at radius values of 0.1μ, 0.3μ and 0.5μ, in the area of transition from Rayleigh to Mie for scattering cross-section. Three groups of curves are shown for the following hygroscopic nucleus substances which may be expected in an urban atmosphere:-

Substance	Molecular Weight (M_1)	Solubility (p) at 273°K
HCl	36.47	82.3 grs per 100 cc of water
NH_4Cl	53.50	29.4
NaCl	58.45	35.7
HNO_3	63.02	Unspecified
H_2SO_4	98.08	Unspecified
$(NH_4)_2SO_4$	132.15	70.6

The specifications quoted may be found in the Handbook of Chemistry and Physics (43rd edition). The curves are derived from equation (6), with extents limited by the solubility consideration described by equation (7).

From these curves it is clear that the nucleus substances NaCl, $(NH_4)_2SO_4$ and NH_4Cl are not effective in the production of solution droplets of radius about 0.3μ until the relative humidity of the atmosphere has risen to above about 80%.

Further, it may be seen that a given hygroscopic nucleus, that is, a certain mass of a certain substance, will tend to come to equilibrium as a solution droplet at a radius which increases as the atmospheric relative humidity increases.

This presentation is merely an extension of work discussed by Mason (1957 and 1962), Robinson (1962) and others.

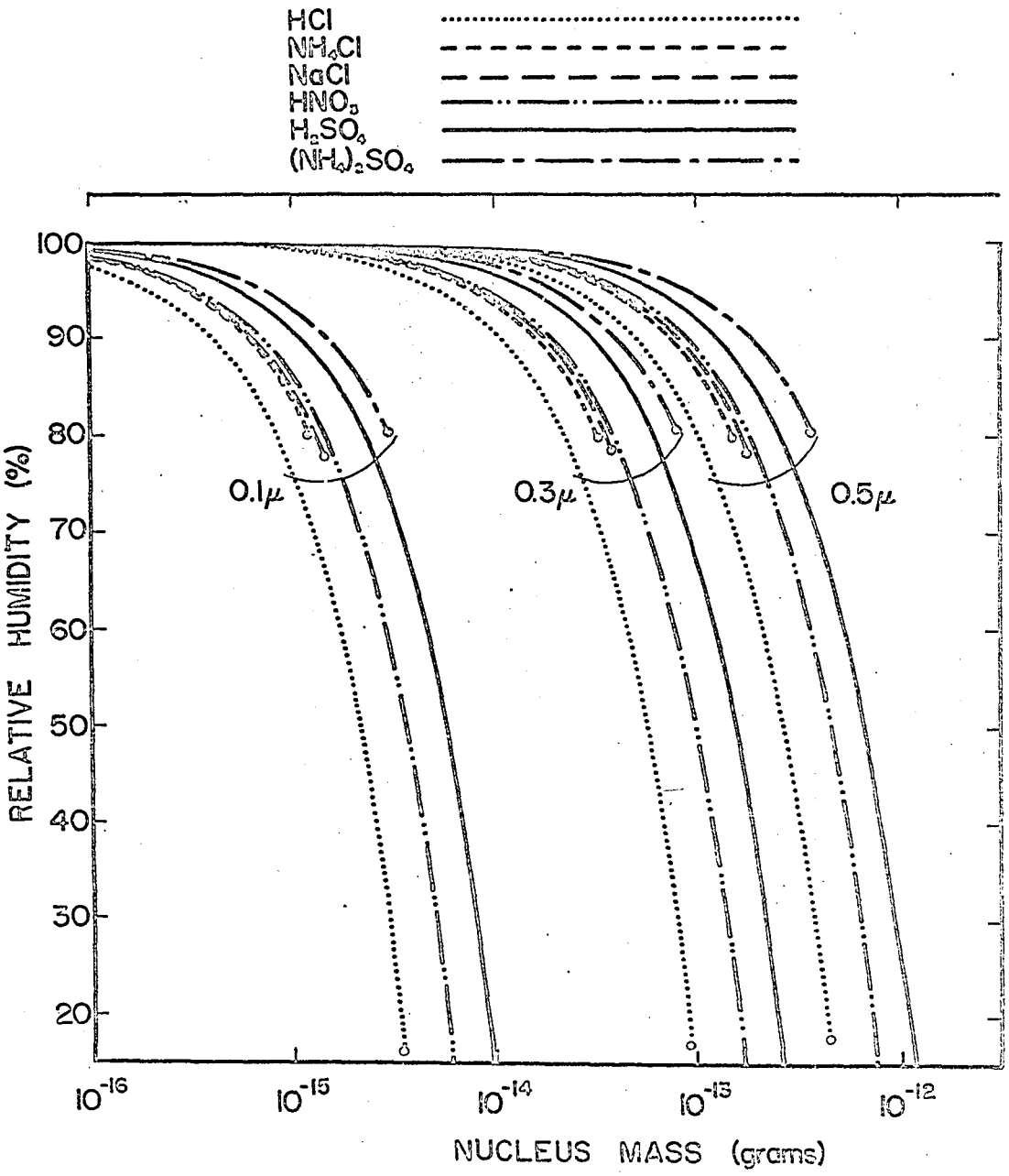

Fig. 17 Equilibrium of solution droplets at radii 0.1, 0.3 and 0.5 μ

Variations of attenuation with relative humidity

Fig. 18 represents about a week's summer data on the effect of changes of relative humidity. Each point represents an hourly measurement so that each day is represented by 24 points. (A few anomalous points have been omitted.) To produce Fig. 18, the sets of 24 points for individual days first were plotted separately; then these plots were superimposed, with displacement relative to one another along the abscissa attenuation scale to give the least scatter (by eye) of the points along this scale. This latter process is justified on the grounds that an average bulb decay effect of about 0.05 db $(7\text{lm})^{-1}$ per day was occurring (see Appendix 2). Further, the water quantity present in the urban atmosphere and the droplet population varies from day to day.

Around 80% relative humidity attenuation increases rapidly with increasing humidity (compare Mason, 1957, Fig. 22, which applies to a site on the coast of Ireland). The change is not sudden, as the deductions of the previous section would imply. However, in summer-time there is no heating of houses in the city and so the quantity of smoke in the atmosphere is relatively small (Summers, 1964); in these circumstances only small numbers of hygroscopic nuclei are to be expected.

Below about 60% relative humidity an average curve for Fig. 18 begins to take a negative slope. This effect is encountered often in the summer. The low humidities generally are associated with sunshine in the middle hours of the day. It is likely that the recurvature phenomenon is an effect of photochemical activity tending to increase the numbers of dilute acid solution droplets by processes of oxidation.

Fig. 17 indicates that such droplets can exist at low relative humidities. This conclusion finds support in work reported by Ahlquist and Charlson (1966). They used an integrating nephelometer to measure hourly values of the scattering coefficient for light in a wavelength range from 0.41 to 0.56μ of small sample volumes of air taken on the campus of the University of Washington, Seattle. Their curve representing the mean diurnal variation of the scattering coefficient for the period 19 July to 18 August 1966 shows a maximum of scattering at around 1100 P.D.T. Their worst day for smog showed a very pronounced maximum of scattering at 1100, accompanied by a peak NO_2 concentration of 0.16 ppm measured at the same site, and a concentration of oxidant in downtown Seattle of 0.15 ppm. This is symptomatic of marked photochemical activity. Los Angeles is famous for this type of smog, and there is an implication here that summer-time Montreal smog is similar. The matter seems to merit further inquiry.

Fig. 19 is a synthesis of representative data on the effect of relative humidity. The zones for the days in April 1967 were made up in a manner similar to that for August 1966 (Fig. 18). The relative humidity scale has here been contracted so that the August data zone (horizontal hatching) appears more compressed than in Fig. 18. The full circle points represent individual observations at several hours both before and after the snowstorm of 29 December 1966; these points are typical of most of the winter's storms, though during the course of a storm the relative humidity commonly rose towards 95%. The crosses and open circles apply to the periods respectively before and

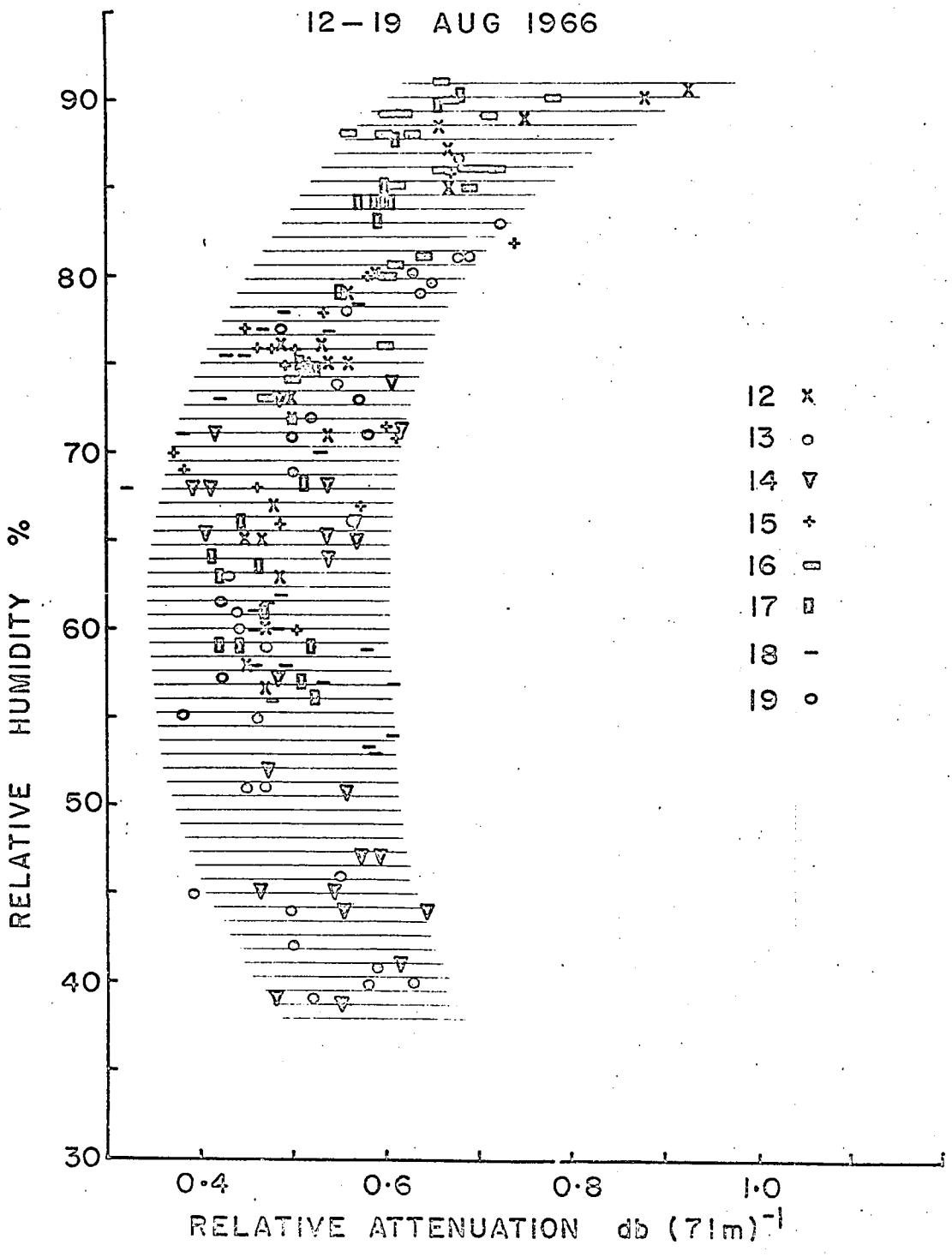

Fig. 18 Dependence of attenuation on relative humidity: 12-19th August 1966

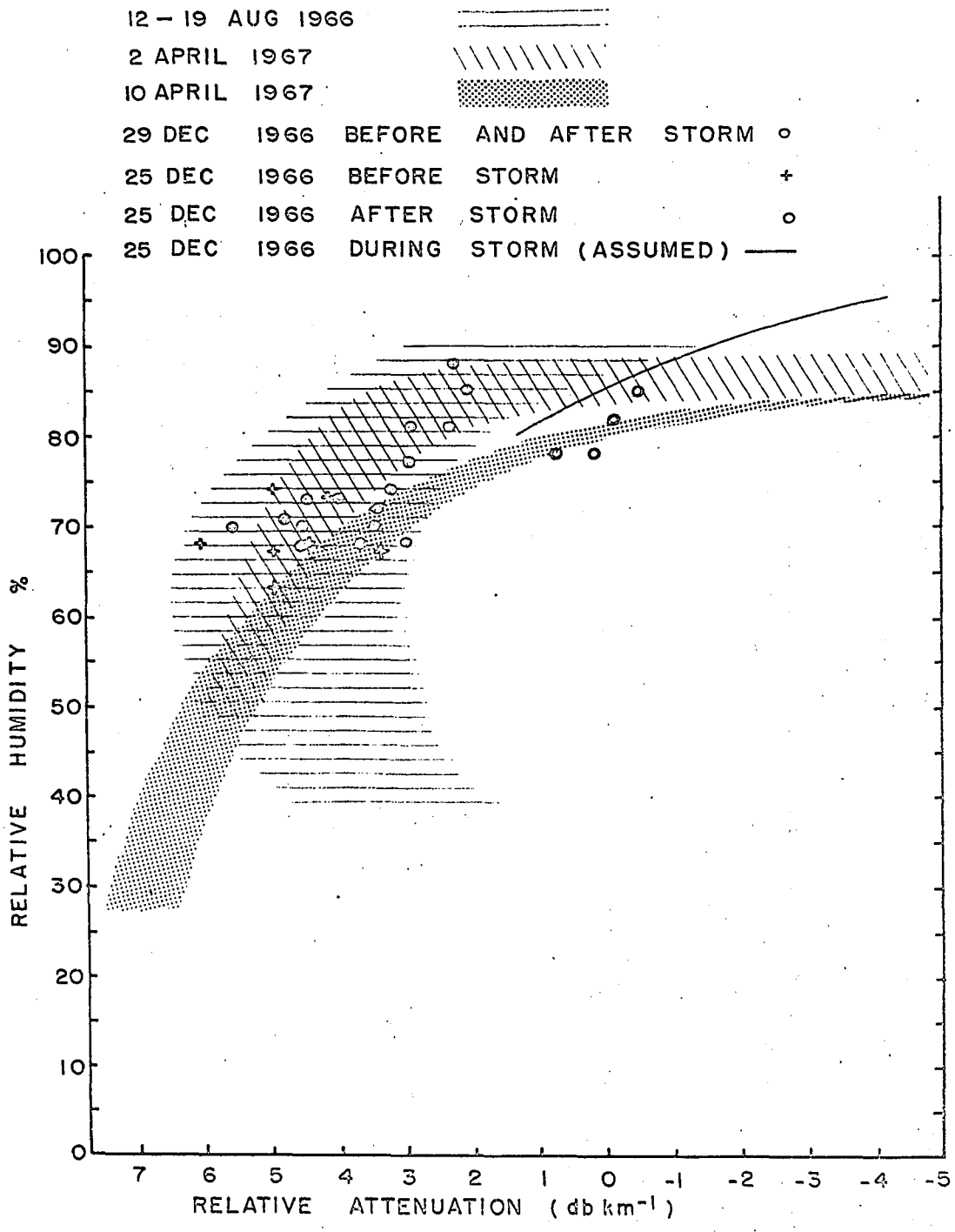

Fig. 19 Dependence of attenuation on relative humidity: typical data combined

after the storm of 25th December. Again for this figure there has been sliding along the abscissa scale to fit together the data from the different times.

There is evident a more marked increase of attenuation with humidity above about 80% than below this level, and it seems appropriate to deduce from the material presented in the previous section that increased numbers of hygroscopic nuclei come into action when the humidity has passed the 80% level.

The solid line has been drawn in on Fig. 19 to model approximately the behaviour of "clear air" attenuation during the Christmas storm, considered in chapter 4, and the abscissa scale in db km^{-1} has been drawn to correspond with this work. In reality attenuation is likely to vary in time in a manner dependent upon the state of evolution of the haze produced by the snowfall. The points on Fig. 19 for 25th December show a wide dispersion between the situations before and after the storm. This might be explained by a change of air mass over the 30 hours of this storm, in which the wind changed from North-east to West and was exceptionally strong.

Appendix 2. Details of the experiment

Fig. 20 illustrates the spectral correspondence between the light source, the photocathode and a filter placed in front of the photocathode as a precautionary measure.

For the purpose of reducing noise in the signal, after early trial experiments, the photoemissive cell was painted with electrically conducting copper paint (Walsco Electronics No. 37-02) so as to provide an electrostatic shield, which was earthed. A small aperture was left unpainted to allow ingress of the light. The use of a Co-netic magnetic shield was found to be not of value in reducing noise.

The photoemissive tube was operated at about 150 volts with a load resistance of 1 megohm so as to yield an approximately linear output at lower attenuations.

The output from the phototube unit was in the form of positive pulses of about 4 volts generated at the cathode of one half of a 12 AT 7 tube, chosen for its comparatively low output impedance. This choice and the use of coaxial cable over the 2' distance between the phototube unit and the amplifier unit overcame capacitance shunting in the output cable.

The pulses were passed through a variable gain voltage amplification stage, then a two-stage peak detector before the final peak reading circuit.

The voltage at the cathode of the triode tube determined the DC current through both of the 1k, 1m.a. chart recorders.

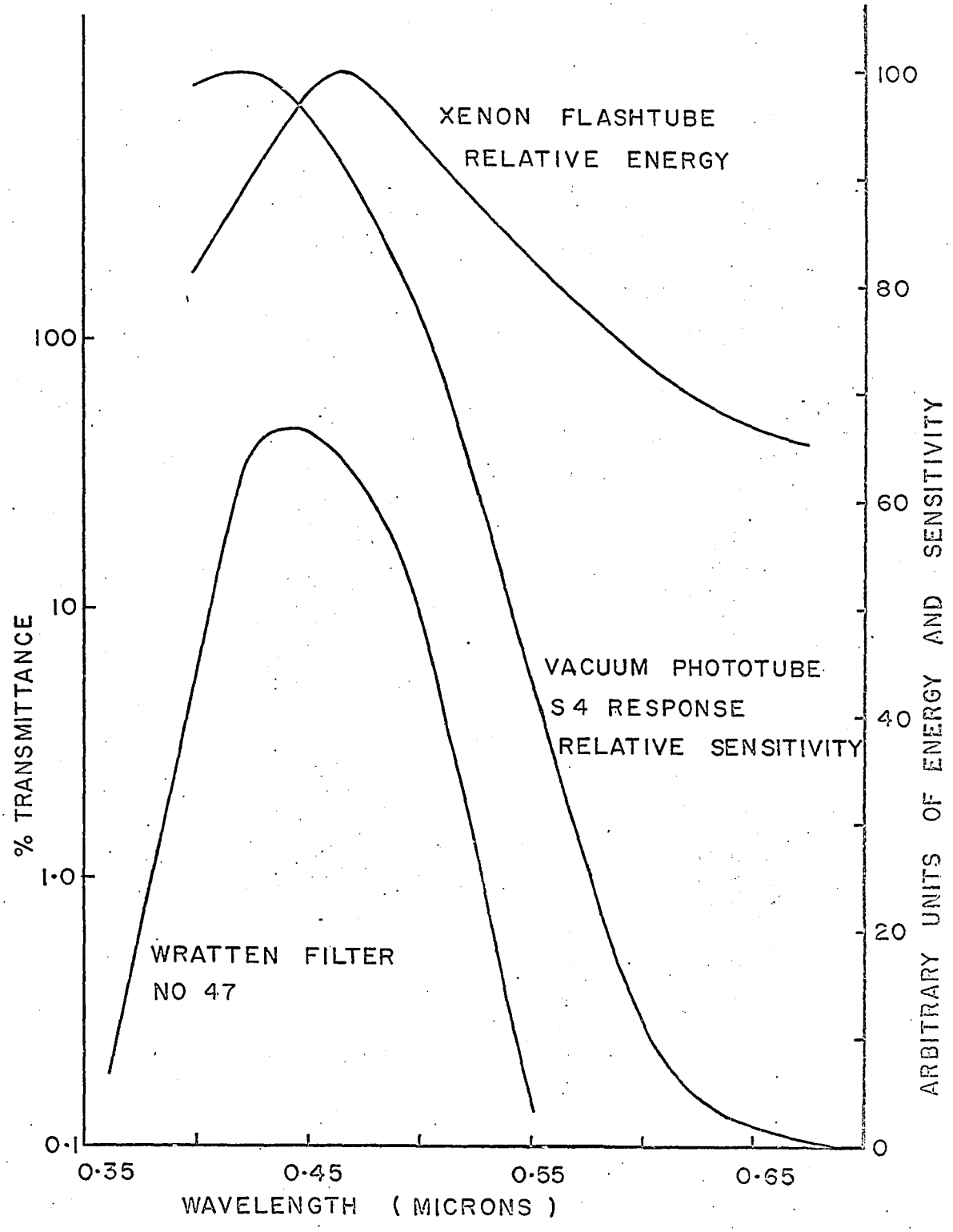

Fig. 20 Spectra of light output, photocathode sensitivity and filter transmissic

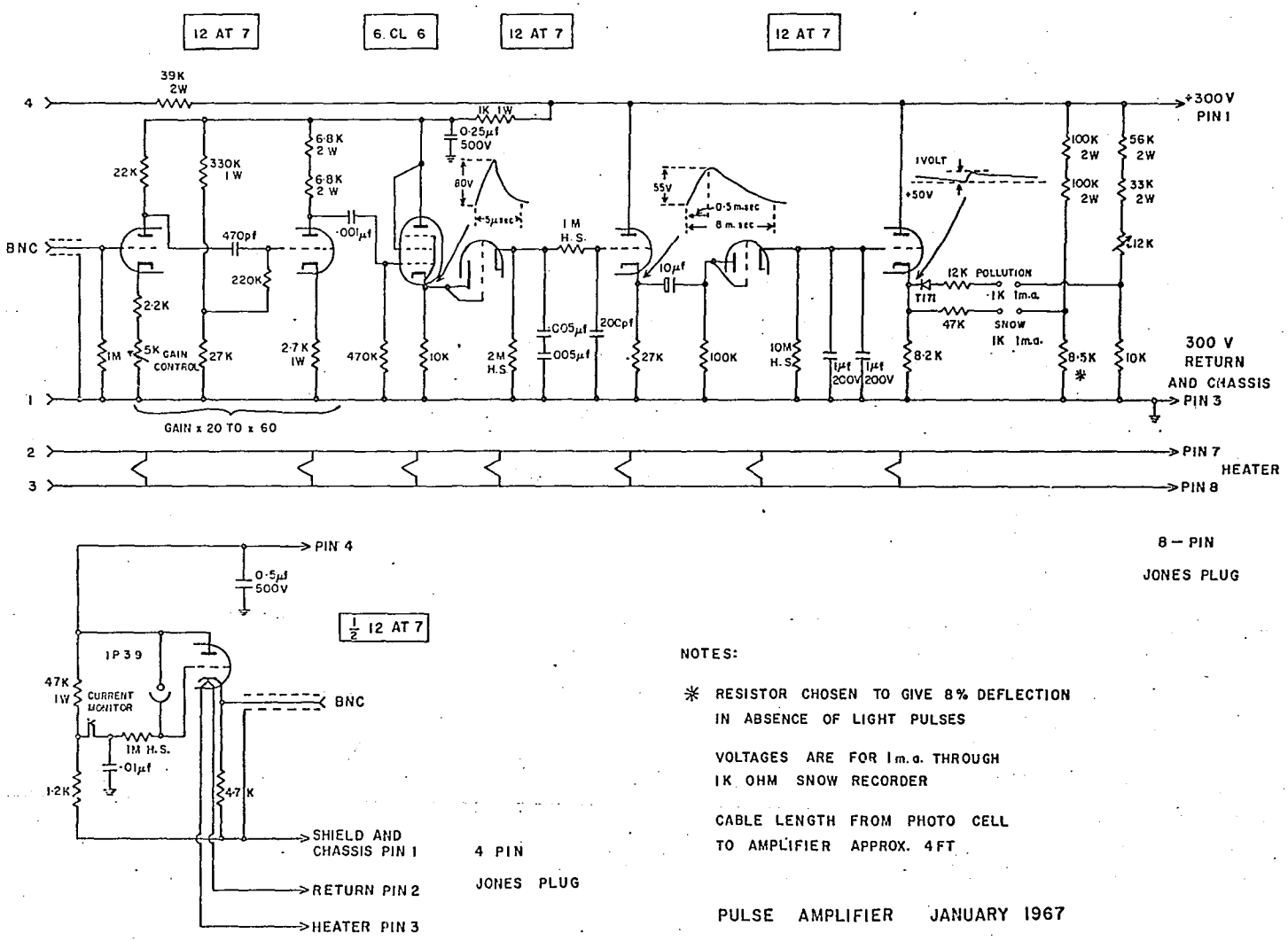

Fig. 21 Circuit diagram

This system was found to operate well over long periods of time, the only difficulties arising from leaks developing in the tubes, and poor electrical contact developing where the leads to the recorders were inserted in sockets in the amplifier chassis.

After 5th January 1967 the number two recorder (labelled "POLLUTION" on the circuit diagram, Fig. 21) was arranged to read attenuations greater than 3 db so that high attenuations could be read with greater accuracy. Prior to that date from 5th August 1966 when recording began, this recorder was set up to read the low attenuations with high resolution, 1.0 db attenuation being sufficient to give a full scale deflection. This was for measurements of atmospheric pollution. Fig. 22 is a typical calibration curve. S_1 refers to the number one recorder, labelled "SNOW" on Fig. 21, and S_2 to the number two. The ordinate is scale divisions of the chart recorder paper and the abscissa is attenuation as introduced by placing Kodak Wratten neutral density filters into the system at the receiver field lens. These filters give attenuations within $\pm 5\%$ of their nominal values, according to the manufacturer, and smooth curves were drawn through calibration points, shown as crosses. Infinite attenuation to give the asymptotes was obtained by covering the receiver aperture. It is seen that the S_1 curve shows high sensitivity at low attenuations, decreasing as the attenuation increases; and that the S_2 curve gives a greater slope and thus higher sensitivity at the high attenuations. In practice the S_2 signal was of value only in determining a peak rate on 11th February 1967, of 8.5 db $(7\text{lm})^{-1}$, or approximately 11 mmw hr^{-1}, occurring over a few

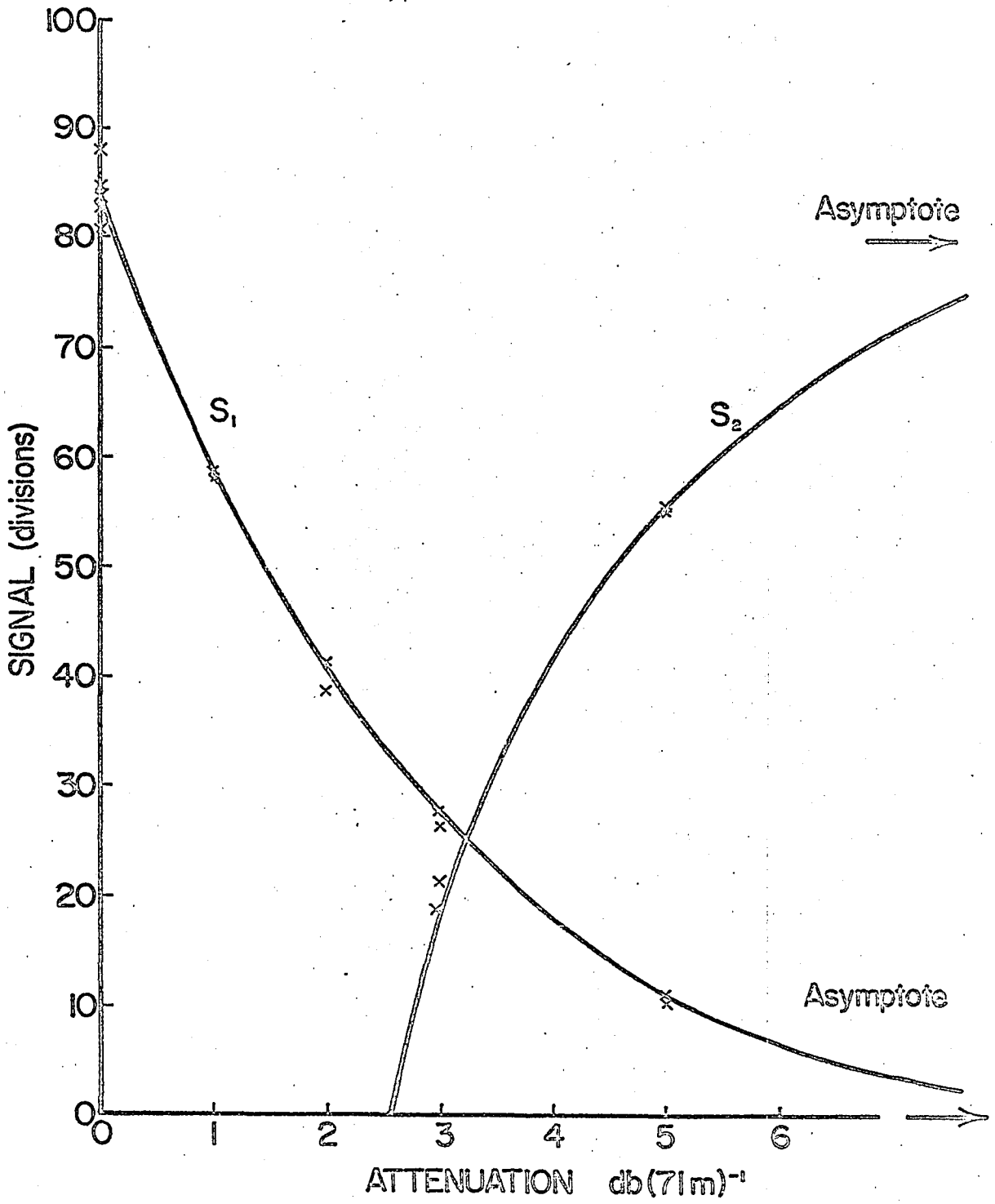

Fig. 22 Typical calibration curves for the transmissometer

minutes. Such calibration operations were carried out at approximately weekly intervals during the season to guard against errors due to changes in the performance characteristics of the instrument components.

The bulb of the Stroboscope light source was found to brown over gradually, leading to a steady reduction of the signal of 1.8 db $month^{-1}$, or 0.05 db day^{-1}. In examination of the records of individual storms, this effect was ignored. It was compensated by occasional alterations of the amplifier gain setting. The Stroboscope bulb was replaced 3 times during the season, and at these times the permanent filters at the receiver field lens were adjusted.

By inclusion in the receiver box of an independent Stroboscope source, it was possible to make tests of the operation of the instrument with the effect of atmospheric changes excluded by blocking the receiver aperture. These tests showed that in normal conditions the trace remained steady within ± 0.02 db.

The effect of changes of temperature on operation at the receiver was tested by opening up both end lids of the receiver box for a period of 10 minutes at night when the air temperature was $-14^{\circ}C$. No discernible effect was seen on the S_1 recorder trace. Earlier laboratory tests of the equipment showed that it was insensitive to temperature changes of a few degrees Centigrade.

The speed of response of the chart recorder pens, after instantaneous changes of the attenuation produced by insertion and removal of filters and blocking off of the receiver aperture, is illustrated in Fig. 23 (Appendix 3). An approximate time constant of the instrument of 10 seconds was obtained. This was felt to be adequate time resolution for the snowfall observations.

Appendix 3. Effects on the recorded trace of smoke plumes and drifting snow.

Fig. 23 shows the last 89 seconds of a 24-minute run made at 3 ins min^{-1} on 15th February 1967. At the time the attenuation was about 9.3 db km^{-1} and snow was falling at about 1 mmw hr^{-1}. On the right is the continuation at 3 in hr^{-1} of normal recording. Over the 15 seconds around 2314 there is a conspicuous peak of attenuation, which corresponds with the numerous spikes seen at 3 in hr^{-1}. During the course of the 24 minute run, the times were recorded of when snow was blown from the roof of the Physics Building across the optical path, and when smoke (or steam) from the chimney of the Otto Maass Chemistry Building drifted across in the north-east wind. Fig. 24 shows the environment of the path. Examination of the recorded trace at 3 in min^{-1} showed that the peaks of attenuation such as that of 2314 could be attributed to either type of obstruction. Thus the blowing snow and steam produced sharp spikes of high attenuation on the trace rather than a steady over-reading. In measuring attenuations, therefore, the effect of these hazards was considered unimportant, as the spiking was easily recognizable and was ignored.

Also plotted out on Fig. 23 are curves of response of the instrument from zero to infinity db $(7lm)^{-1}$ and from five to infinity db $(7lm)^{-1}$. It is notable that where the attenuation is increasing sharply the shape of the trace follows that of the response curve. Thus the noise on the trace was determined by the time constant of response of the instrument, which was of the order of 10 seconds.

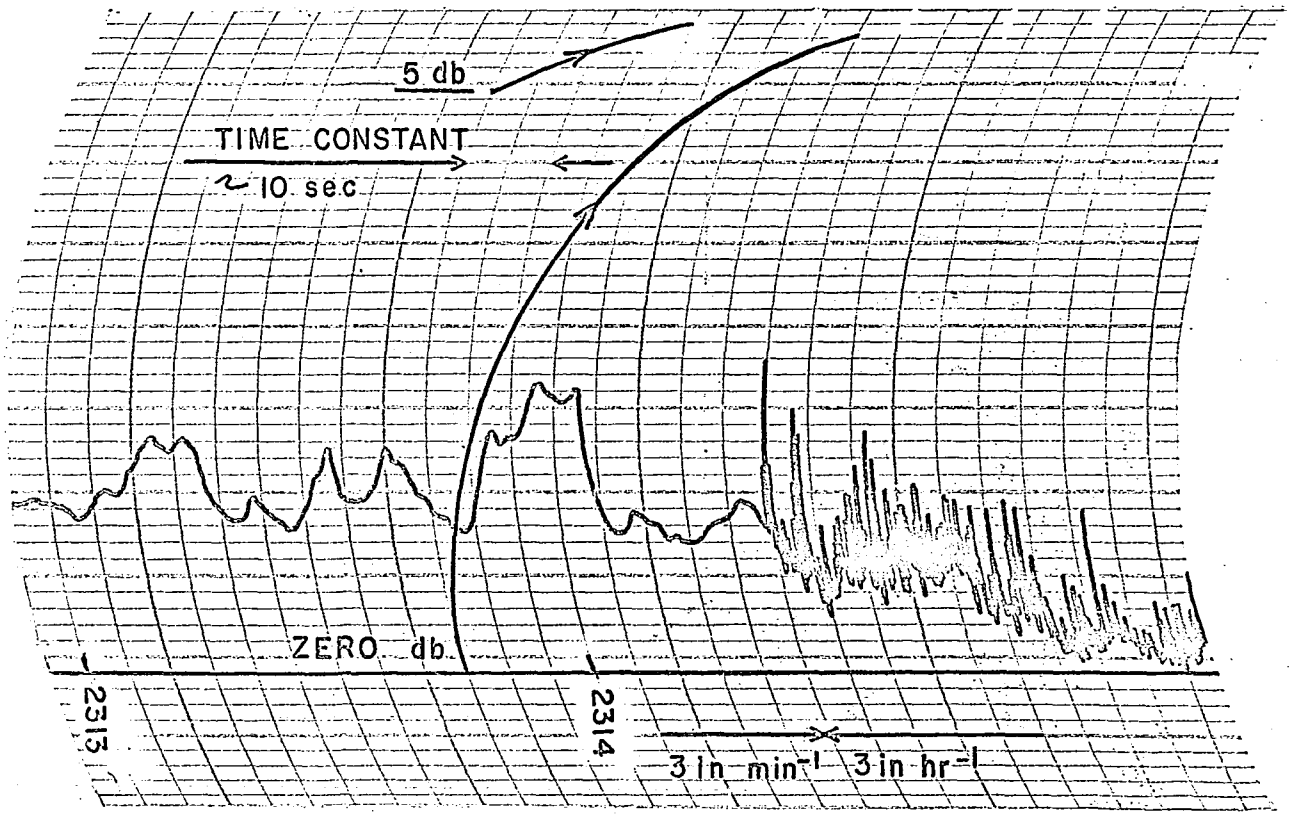

Fig. 23 Trace recording at 3 in min^{-1} on 15th February 1967

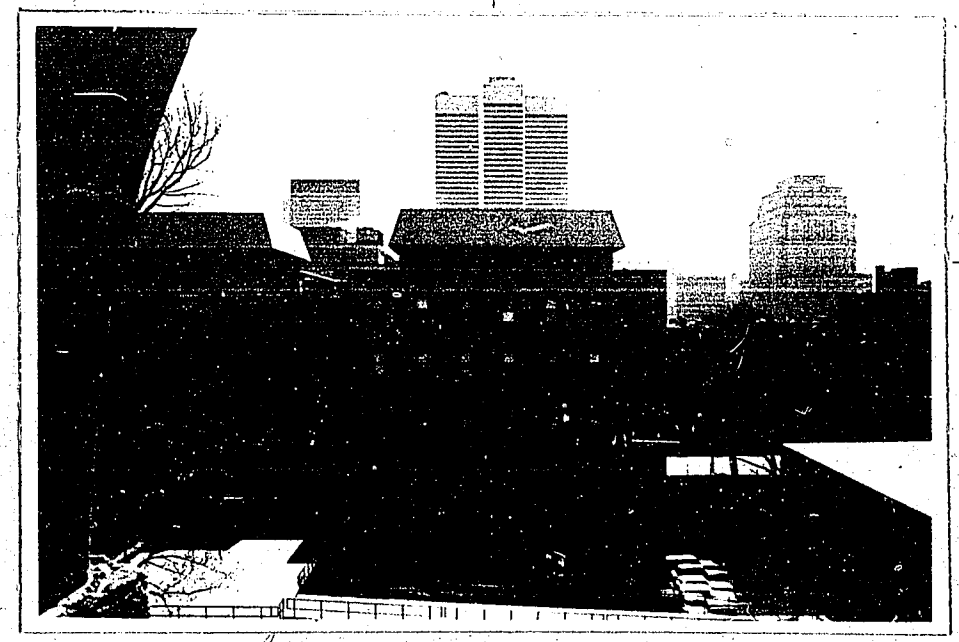

TRANSMITTER

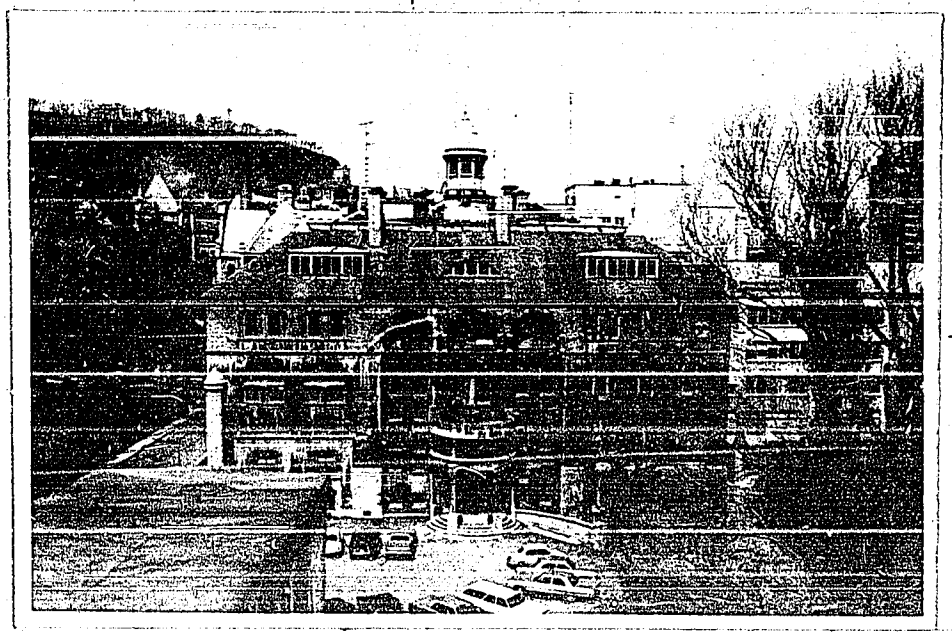

RECEIVER

Fig. 24 The environment of the optical path

TRANSMITTER

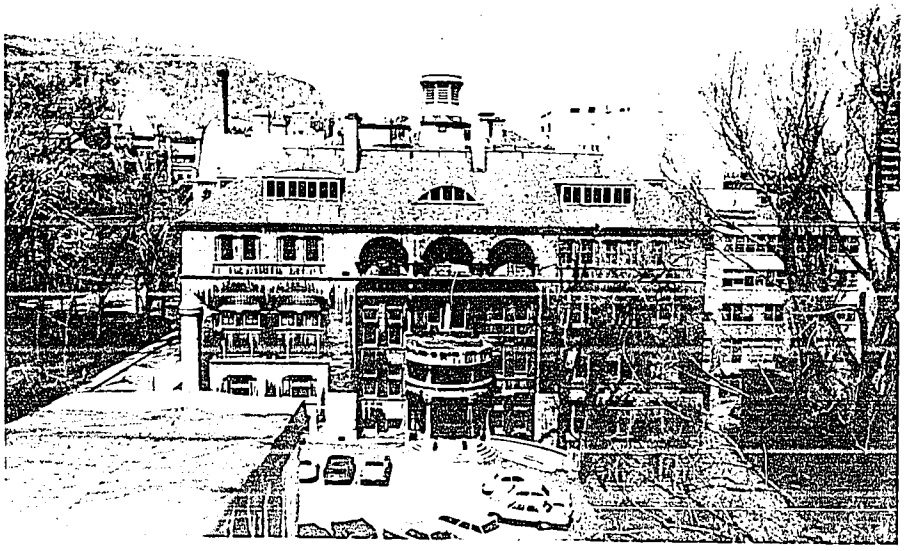

RECEIVER

Fig. 24 The environment of the optical path

Appendix 4. Comparison with the Department of Transport transmissometer at Dorval Airport

The D.O.T. transmissometer was manufactured by the Crouse-Hinds Company, Syracuse 1, N.Y. Mounted on concrete bases about 5 m above ground level, the transmitter and receiver were separated by a 185-m path. The transmitted light came from a tungsten filament sealed reflector lamp having a wide angle beam, and a refracting telescope was used to focus this steady light on to the cathode surface of a photoemissive cell (Cetron Electronic Corporation type CE 75 V) having an S1 response with a peak of sensitivity in the infra-red. The receiver aperture was varied upwards towards a maximum of 10.2 cm according to the light output. The receiver field of view was 0.13° and the transmitter was situated North of the receiver, so that the current due to skylight was negligible. The steady current through the phototube charged a capacitor until the voltage across its plates was sufficiently great to trigger a thyratron tube, whereupon the process repeated. The rate of firing of the thyratron tube yielded a measure of the amount of light transmitted. The principle of operation involved thus differed from that of measurement of voltage pulses used in the work reported here.

The results obtained by the two systems were similar during the 1966-67 snowfall season. Calibration was based on the assumption that the transmission of the atmosphere varied linearly with the signal on the D.O.T. transmissometer trace. On this basis it was possible to compare attenuations recorded by each transmissometer at the same time. Fig. 25 shows corresponding recorded traces from Dorval and McGill for the 16 hours of the storm of 29th December 1966. The

variations on the trace are more prominent on the Dorval record because of the smaller dynamic range of that instrument. Over the Christmas storm the Dorval instrument showed saturation with the snowfall rate above about 3 mmw hr^{-1}. Here the mean rate was 1.6 mmw hr^{-1}. The larger fluctuations on the McGill trace probably were due to a shorter time constant.

Comparison of maxima and minima shows that the Dorval record lags the McGill record on the average by 7 minutes. Taking account of this, half hour mean attenuations were compared, and 29 points for the interval 0100 to 1530 were plotted to produce Fig. 26. The separation of the two instruments was about 9 miles, and the site locations were of different character; the McGill transmissometer path was about 20 m above ground level in an urban environment, and the Dorval instrument path was a few metres above the surface of the airfield. The beam volume of the McGill instrument was about 4 m^3 and that of the Dorval instrument about 15 m^3 (with the receiver aperture at 10.2 cm). In view of these differences, it is seen that there is good agreement between the two systems.

The dominant wavelength for the Dorval instrument was about 0.75μ (given by the S1 response curve), and it is to be expected that at this wavelength the effect of relative humidity will not be of as great importance as it is for the McGill instrument (see chapter 5). On Fig. 25 it is apparent that there is unexpectedly a lower attenuation level at the end of the storm than at the beginning, about 2.0 db km^{-1} less; this contrasts with an increase of about 2.4 db km^{-1} on the McGill record. It is thought that differences in light smog are responsible for this discrepancy.

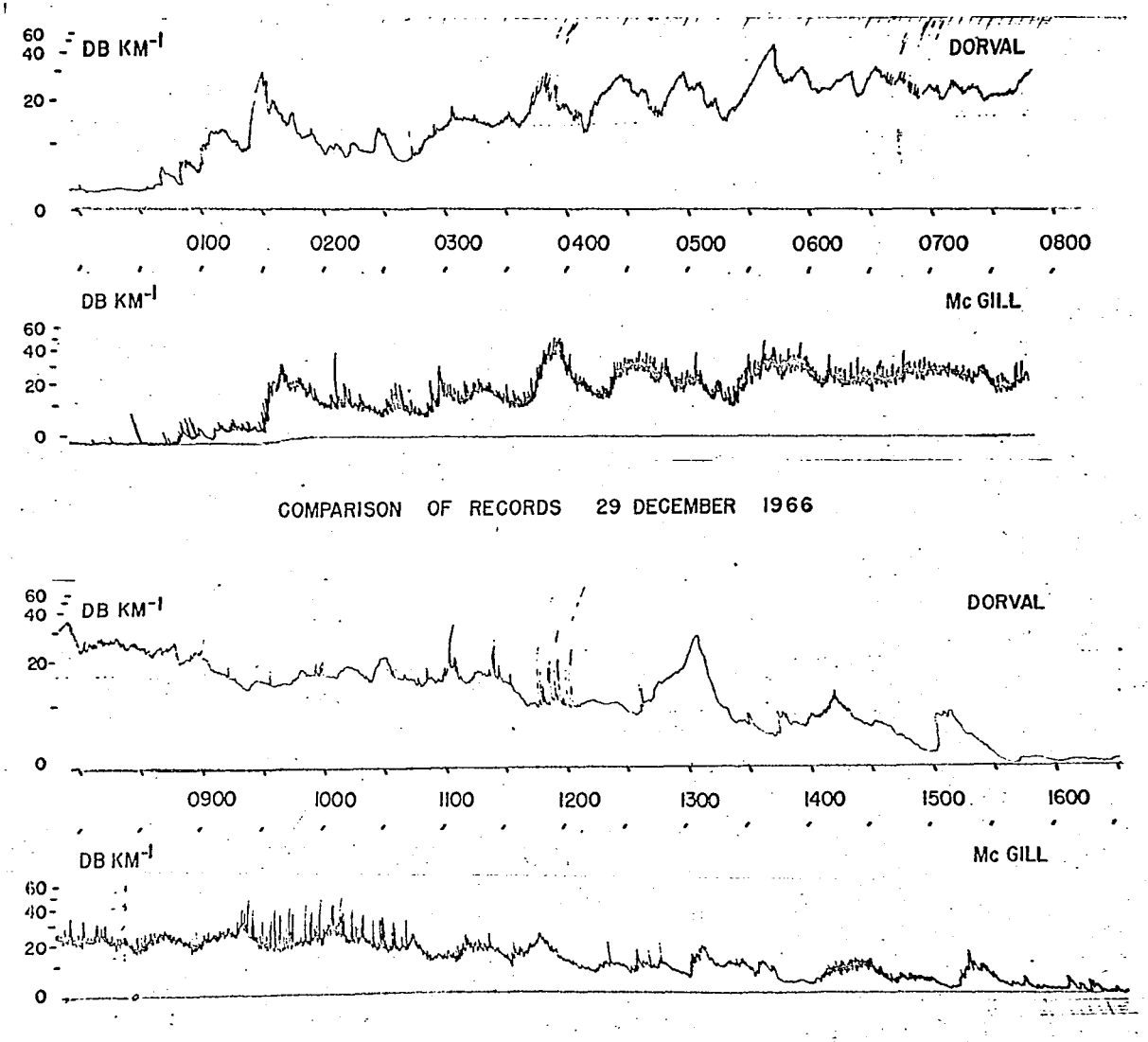

Fig. 25 Comparison of recordings of the Dorval and McGill instruments (29th December 1966)

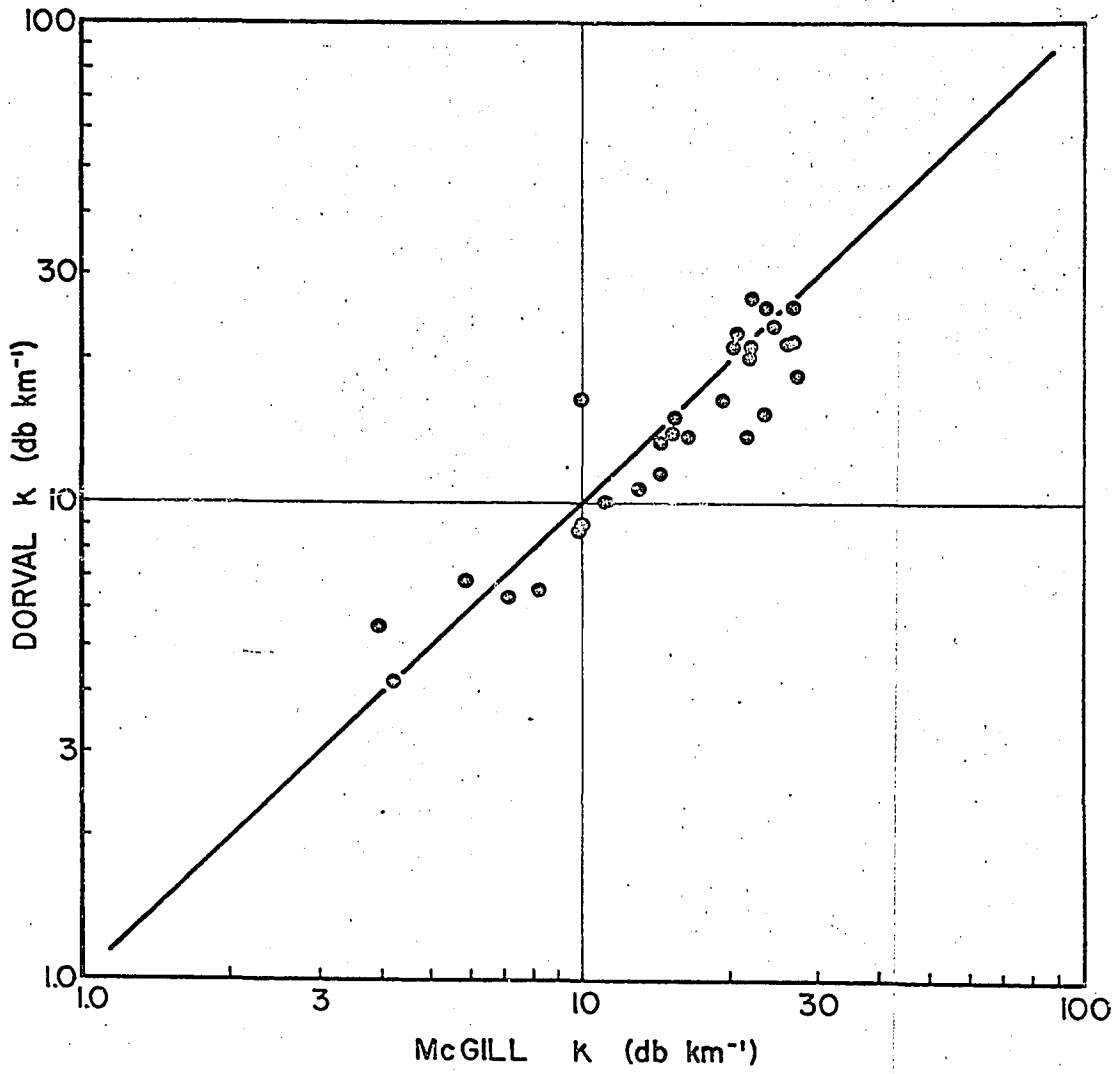

Fig. 26 Comparison of half-hour mean attenuations (29th December 1966)

REFERENCES

Ahlquist, N.C. and R.J. Charlson, 1966: A new instrument for evaluating the visual quality of air. A paper presented at the Annual Meeting of the Pacific Northwest International Section of the Air Pollution Control Association, Seattle, Washington, 3-4 November, 1966.

Andrews, J.F., 1967: The circulation and weather of 1966. Weatherwise, 20, I, 7-15.

Arnulf, A., J. Bricard, E. Curé and C. Véret, 1957: Transmission by haze and fog in the spectral region 0.35 to 10 microns. J. Opt. Soc. Amer., 47, 491-498.

Deirmendjian, D., 1962: Rand Corp. Mem. RM-3228-PR. Page 9.

Eldridge, R.G., 1966: Haze and fog aerosol distributions. J. Atmos. Sci., 23, 605-613.

Fletcher, N.H., 1962: The Physics of Rainclouds. Cambridge, University Press, 386pp.

Gunn, K.L.S., 1965: Measurements on new fallen snow. McGill University Stormy Weather Group Scientific Report MW-44.

Gunn, K.L.S. and J.S. Marshall, 1958: The distribution with size of aggregate snowflakes. J. Meteor., 15, 452-461.

Langleben, M.P., 1954: The terminal velocity of snow aggregates. Quart. J.R. Meteor. Soc., 80, 174-181.

Lillesaeter, O., 1965a: Attenuation of a parallel beam of light, particularly by snow. McGill University Stormy Weather Group Scientific Report MW-43.

Lillesaeter, O., 1965b: Parallel-beam attenuation of light, particularly by falling snow. J. Appl. Meteor., 4, 607-613.

Mason, B.J., 1957: The Physics of Clouds. Oxford, Clarendon Press, 481pp.

Mason, B.J., 1962: Clouds, Rain and Rain making. Cambridge, University Press, 145pp.

Middleton, W.E.K., 1952: Vision Through the Atmosphere. University of Toronto Press, 250pp.

Robinson, Elmer, 1962: Air Pollution, Vol. I. (Arthur C. Stern, ed.) New York and London, Academic Press. 656pp.

Stewart, H.S. and R.F. Hopfield: Applied Optics and Optical Engineering, Vol. I. (R. Kingslake, ed.) New York and London, Academic Press, 423pp.

Summers, P.W., 1964: An Urban Ventilation Model Applied to Montreal. Ph.D. Thesis, McGill University.

Van de Hulst, H.C., 1957: Light Scattering by Small Particles. New York, Wiley, 470pp.